Bacterial vaginosis-driven changes in vaginal T cell phenotypes and their implications for HIV susceptibility

Finn MacLean[1], Adino Tesfahun Tsegaye[2], Jessica B. Graham[1], Jessica L. Swarts[1], Sarah C. Vick[1], Nicole Potchen[1], Irene Cruz Talavera[1], Lakshmi Warrier[1], Julien Dubrulle[3], Lena K. Schroeder[3], Corinne Mar[2], Katherine K. Thomas[2], Matthias Mack[4], Michelle C. Sabo[5], Bhavna H. Chohan[2,6], Kenneth Ngure[2,7], Nelly Mugo[2,8], Jairam R. Lingappa[2,5,9*], Jennifer M. Lund[1,2*] for the Kinga Study Team

[1]Vaccine and Infectious Disease Division, Fred Hutchinson Cancer Center, Seattle, USA

[2]Department of Global Health, University of Washington, Seattle, USA

[3]Cellular Imaging Shared Resource, Fred Hutchinson Cancer Research Center, Seattle, USA

[4]Department of Internal Medicine-Nephrology, University Hospital Regensburg, Regensburg, Germany

[5]Department of Medicine, University of Washington, Seattle, USA

[6]Center for Virus Research, Kenya Medical Research Institute, Nairobi, Kenya

[7]School of Public Health, Jomo Kenyatta University of Agriculture and Technology, Nairobi, Kenya

[8]Center for Clinical Research, Kenya Medical Research Institute, Nairobi, Kenya

[9]Department of Pediatrics, University of Washington, Seattle, USA

*Contributed equally

Corresponding Authors:

Jennifer M. Lund

1100 Fairview Ave N., E5-110

Seattle, WA 98109

+1-206-667-2217

jlund@fredhutch.org

Jairam R. Lingappa

908 Jefferson St, Box 359927

Seattle, WA 98104

+1-206-520-3822

lingappa@uw.edu

Abstract

Bacterial vaginosis (BV) is a dysbiosis of the vaginal microbiome that is prevalent in reproductive-age women worldwide. Adverse outcomes associated with BV include an increased risk of sexually acquired Human Immunodeficiency Virus (HIV), yet the immunological mechanisms underlying this association are not well understood. To investigate BV driven changes to cervicovaginal tract (CVT) and circulating T cell phenotypes, participants with or without BV provided vaginal tract (VT) and ectocervical (CX) tissue biopsies and peripheral blood mononuclear cells (PBMC). Immunofluorescence analysis of genital mucosal tissues revealed a reduced density of $CD3^+CD4^+CCR5^+$ cells in the VT lamina propria of individuals with compared to those without BV (median 243.8 cells/mm^2 BV- vs 106.9 cells/mm^2 BV+, p=0.043). High-parameter flow cytometry of VT biopsies revealed an increased frequency in individuals with compared to those without BV of dysfunctional $CD39^+$ conventional $CD4^+$ T cells (Tconv) (median frequency 15% BV- vs 30% BV+, p_{adj}=0.0331) and tissue-resident $CD69^+CD103^+$ Tconv (median frequency 24% BV- vs 38% BV+, p_{adj}=0.0061), previously reported to be implicated in HIV acquisition and replication. Our data suggests that BV elicits diverse and complex VT T cell alterations and expands on potential immunological mechanisms that may promote adverse outcomes including HIV susceptibility.

Introduction

Bacterial vaginosis (BV) is characterized by a vaginal dysbiosis in which the normally *Lactobacillus*-dominated microbiome is replaced by one with higher bacterial diversity, including increased concentrations of anaerobic bacteria (1). BV results in symptoms of vaginal inflammation, discharge, and discomfort, and is estimated to affect 23-29% of reproductive-age women worldwide (2), making BV the most common cause of vaginal symptoms leading patients to seek medical care (3). BV is also associated with several adverse medical outcomes (1, 2, 4-11) including preterm delivery (12), chorioamnionitis (13), endometritis (14), and an increased risk of Human Immunodeficiency Virus (HIV) acquisition (5, 11). The issue of HIV acquisition risk is of particular concern in parts of the world where BV and HIV are individually prevalent, as is the case in sub-Saharan Africa (15). Although many studies have investigated immune system alterations associated with BV (1, 5-7, 10, 11, 16-19), the link between cervicovaginal tract (CVT) T cells, which may mediate the relationships between BV and adverse outcomes, is not well understood. Here, we sought to better understand the impact of BV on CVT mucosal and systemic immune responses in Kenyans and how these changes may alter HIV susceptibility.

In the CVT, innate and adaptive immune cells line the epithelium and lamina propria to provide immunological surveillance (20). Notably, T cell populations in the CVT maintain distinct phenotypes from those circulating in the blood (21, 22). These include tissue-resident memory T cells (T_{RM}) bearing CD69 with or without CD103 (23). CD69 is a marker of activation (24) that has a unique role in maintaining tissue residency by binding S1PR1 and preventing egress from the tissue (25-27). CD103 further promotes tissue residency by binding to E-

cadherin (28). T_{RM} are retained in the mucosal tissue and have the ability to readily respond to pathogens *in situ* (21, 29-31). Upon recognition of their cognate antigen, T_{RM} use their "sensing and alarm function" to produce pro-inflammatory cytokines and chemokines that rapidly recruit and activate other immune cells, thereby potentiating the tissue immune response while also executing their specific effector and cytotoxic functions (32-35).

Given that CVT mucosal tissue is the site where, in the context of heterosexual transmission, HIV exposure first occurs, activated $CD4^+$ T cells expressing the HIV coreceptor CCR5 in the CVT have been thought to be prime targets for initial HIV infection (36). Studies using a mouse model demonstrated that the introduction of BV-associated bacteria into the vagina led to an increased quantity of CVT $CD4^+$ T cells expressing the activation marker CD44 and HIV coreceptor CCR5 (7), suggesting dysbiosis of normal vaginal flora may lead to an increase of HIV target cells. In humans, studies of immune responses in context of BV have characterized immune cells collected from the CVT lumen via minimally invasive sampling techniques such as cervicovaginal lavage, vaginal swabs, cervical swabs, or cytobrushes. These studies have identified an increase in $CCR5^+CD4^+$ T cells in the CVT lumen of BV+ individuals (37-40), without addressing whether this observation is true in the CVT deeper tissue layers. In addition to the detection of HIV target cells in the CVT lumen of individuals with BV, studies have shown a connection between BV and the presence of pro-inflammatory cytokines in the CVT, most reliably IL-1β (7, 37, 41, 42); adding further support to the idea that proinflammatory mechanisms underlie the link between BV and increased HIV susceptibility. However, the relationship between BV and an increase in $CD4^+$ T cell activation is inconsistently observed (43, 44), suggesting more complex mechanisms may be contributing to increased HIV susceptibility in individuals with BV. Further characterizing BV driven immune modulations in

the unique immune environment of the CVT is paramount to understanding mechanisms underlying increased HIV susceptibility in BV+ individuals.

To comprehensively evaluate immune alterations associated with BV, we utilized tissue cryopreservation (45) and high-parameter, high-throughput flow cytometry to compare immune cells isolated from CVT tissue biopsies and blood collected from individuals with versus without BV. Given the dense T cell populations within CVT tissue (46), cells isolated from CVT mucosal biopsies may better represent the mucosal tissue immune environment than those isolated from the CVT lumen by cytobrush or other methods. Additionally, improved flow cytometry technology allows us to broadly evaluate immune cells in the context of BV for phenotypic markers not previously characterized.

Here, we report detailed T cell characteristics of vaginal tract (VT) and ectocervix (CX) mucosal tissues and peripheral blood mononuclear cells (PBMC) from the same participants, comparing those individuals with to those without BV. Additionally, we analyzed CVT fluids and serum for local and systemic cytokines and chemokines in individuals with versus without BV. While we did not find an increase in $CD3^{+}CD4^{+}CCR5^{+}$ HIV target cells in the CVT of BV+ individuals, we did observe VT T cells with dysfunctional phenotypes and altered expression of soluble mediators in CVT fluid from BV+ individuals. Our findings highlight additional mechanisms not previously entertained that may underlie increased HIV susceptibility associated with BV.

Results

Study population characteristics

Of the 245 Kinga Study participants with analyzed samples, 212 participants met the criteria to be included in the BV flow cytometry analysis. 64 participants contributed samples when they were BV+ by Nugent score (46 at study enrollment and 18 at study exit). The BV-comparator group was comprised of samples contributed by the remaining N=148 participants who had normal flora at enrollment. Overall, our study population was young (57% were <30 years of age), sexually active (median of 8 unprotected sex acts in the prior month), with 40% using hormonal contraceptives, 39% HSV-2 seropositive, and 17% had a sexual partner living with HIV (**Table 1**). Analysis for soluble immune factors was performed on a subset of these participants (N=130 BV-, N=57 BV+). Similarly, immunofluorescent imaging was performed on a smaller subset (N=55 VT BV-, N=18 VT BV+, N=44 CX BV-, N=16 CX BV+).

Reduced abundance of $CCR5^+$ HIV target cells in the VT lamina propria in individuals with BV

It has been reported that T cells are distributed throughout the epithelium and lamina propria tissue compartments in the CVT with great abundance in the lamina propria space bordering the epithelium (46). To quantify how $CD3^+CD4^+CCR5^+$ HIV target cell density in both the epithelium and lamina propria is affected by BV, we performed immunofluorescent staining on CX and VT tissue sections from individuals with versus without BV. The epithelium and lamina propria were visualized by H&E staining **(Fig 1a)** or were labeled with immunofluorescent antibodies against CD3, CD4, and CCR5 and counterstained with DAPI **(Fig 1b)** for T cell density quantification. We found the density of $CD3^+$ and $CD3^+CD4^+$ cells in the

VT lamina propria were not significantly different between BV+ and BV- individuals **(Fig 1c)**; however, we observed a significant reduction in $CD3^+CD4^+CCR5^+$ HIV target cells in the VT lamina propria (median 243.8 cells/mm^2 BV- vs 106.9 cells/mm^2 BV+, p = 0.043; **Table S2.1**) in samples from BV+ compared to BV- individuals **(Fig 1c)**, with minimal differences observed in the VT epithelium **(Fig 1d)**. In contrast, no significant differences in $CD3^+$, $CD3^+CD4^+$, or $CD3^+CD4^+CCR5^+$ cell densities were observed in the lamina propria or epithelium of CX tissue sections from BV+ individuals compared to BV- individuals (**Fig 1e-f, Table S2**).

$CD8^+$ T cells are enriched in the VT of individuals with BV

To investigate the CVT mucosal T cell population in greater detail, we performed high-parameter flow cytometry on cells isolated from cryopreserved CX, VT, and PBMC samples. The majority of $CD45^+$ cells in the VT and CX are $CD3^+$ T cells (median > 75%; **Fig 2a**, **Table S3.1-2)** demonstrating the importance of T cells in immunosurveillance of the CVT. More significant phenotypic T cell differences were observed when VT samples from BV+ vs BV- participants were compared, and fewer differences were observed in either the CX or PBMC (**Table S3**), underscoring that major alterations in T cell populations in the context of BV may be specific to the VT. More specifically, we evaluated $CD3^+$ T cell frequency as a fraction of $CD45^+$ cells and found significantly greater $CD3^+$ T cell frequency in VT samples (median frequency 77% BV- vs 83% BV+, p_{adj} = 0.0485; **Table S3.1**) from BV+ compared to BV- individuals (**Fig 2a**). The fraction of $CD3^+$ T cells with a conventional $CD4^+$ T cell (Tconv) phenotype ($CD4^+CD25^-$; **Figure S1**) among total $CD45^+$ cells was not significantly altered by BV status (**Fig 2b**), but the frequency of $CD8^+$ T cells among $CD45^+$ cells was significantly increased (median frequency 30% BV- vs 38% BV+, p_{adj} = 0.0041; **Table S3.1**) in the VT of

individuals with vs without BV (**Fig 2c**), suggesting that $CD8^+$ T cells are enriched in VT samples from BV+ compared to BV- individuals and may be driving a total increase in VT T cells in BV+ individuals. When evaluating the frequency of Tconv cells as a fraction of total $CD3^+$ T cells, we observed a significant decrease in VT samples (median frequency 44% BV- vs 32% BV+, $p_{adj} = 0.018$; **Table S3.1**) from BV+ individuals compared to BV- individuals (**Fig 2d**). Consequently, we observed a significantly increased $CD8^+$ T cell fraction of total T cells in VT samples (median frequency 38% BV- vs 44% BV+, $p_{adj} = 0.0075$; **Table S3.4**) from BV+ vs BV- individuals (**Fig 2e**). The enrichment of $CD8^+$ T cells in the VT of BV+ individuals appears to be associated with higher total T cell frequency, as well as a shift in $CD4^+/CD8^+$ T cell ratio in the VT of BV+ individuals.

Few phenotypic alterations in CVT or circulating $CD8^+$ T cells in individuals with BV

To further investigate the enriched $CD8^+$ T cell subset in the VT of BV+ individuals, we evaluated $CD8^+$ T cells for differences in activation markers comparing BV+ vs BV- individuals. Overall, we found very few differences in $CD8^+$ T cell phenotypes in the CX, VT, or PBMC of individuals with vs without BV (**Table S3.4-6**). Notably, we observed a significantly lower frequency of the activated phenotype (47) HLA-DR^+CD38^+ $CD8^+$ T cells in the VT (median frequency 2.0% BV- vs 0.9% BV+, $p_{adj} = 0.0309$; **Table S3.4**) of BV+ compared to BV- individuals (**Fig 3a**), possibly indicating a reduction in $CD8^+$ T cell activation in dysbiotic VT tissues. Additionally, we evaluated Granzyme B as a measure of the cytotoxic potential of $CD8^+$ T cells (48) and found no significant differences in the frequency of Granzyme B^+ $CD8^+$ T cells (**Fig 3b**) or any other $CD8^+$ T cell activation marker comparing BV+ and BV- individuals, (**Table S3.4-6**).

Next, we evaluated $CD103^+CD69^+$ co-expression on $CD8^+$ T cells as markers indicative of T_{RM} (24, 46). We hypothesized that $CD8^+$ T_{RM} would play a critical role in immune modulations associated with BV but found that $CD69^+CD103^+$ expression on $CD8^+$ T cells was not differentially expressed in BV+ vs BV- individuals in any of the tissue compartments (**Fig 3c**). In addition to canonical T_{RM} markers CD69 and CD103, we also stained for CD101, another marker associated with the tissue memory T cell signature (23). Similar to CD69 and CD103 expression, we observed no differences in the frequency of $CD101^+$ $CD8^+$ T cells in BV+ vs BV- individuals (**Fig 3d**). Our data suggests that, while $CD8^+$ T cells comprise the majority of T cells in the VT of BV+ individuals, there is little difference in their cytotoxic potential, tissue-resident signature, or other functional markers compared with $CD8^+$ T cells from BV- individuals.

Conventional $CD4^+$ T cells display signs of dysfunction in VT of individuals with BV

To evaluate whether the reduced Tconv frequency among total T cells in the VT of BV+ individuals (**Fig 2d**) was related to differences in markers of effector function, we examined a wide range of phenotypic markers on Tconv, as we did for $CD8^+$ T cells (**Table S3.7-9**). We found $CD39^+$ frequency significantly increased on Tconv cells in VT samples from BV+ individuals (median frequency 15% BV- vs 30% BV+, $p_{adj} = 0.0331$; **Table S3.7**), with minimal differences observed in the CX and PBMC samples (**Fig 4a**). CD39 is a marker of metabolic stress (49) and may contribute to Tconv dysfunction in the VT of BV+ individuals.

Additionally, we found a statistically significant decrease in the frequency of TCF-1^+ Tconv in the VT of BV+ compared to BV- individuals (median frequency 30% BV- vs 24% BV+, $p_{adj} = 0.041$; **Table S3.7**), with no significant differences in the CX or PBMC (**Fig 4b**). TCF-1 is a stabilizing transcription factor implicated in the regulation of progenitor potential and

promotion of T cell fate specification (50-56). Thus, our data suggests that Tconv cells in the VT of BV+ individuals have a reduced capacity to undergo differentiation or serve as proliferative progenitor cells.

Conventional CD4$^+$ T cells display increased markers of tissue residency in VT samples from individuals with BV

Next, we analyzed tissue resident phenotypes in Tconv cells in all three sample types. We found a significant increase in CD69$^+$CD103$^+$ frequency of Tconv cells in VT from BV+ compared to BV- individuals (median frequency 24% BV- vs 38% BV+, p_{adj} = 0.0061; **Table S3.7**), with no differences observed in the CX or PBMC (**Fig 4c**). The frequency of CD69$^+$CD103$^+$ Tconv was enriched in both the VT and CX compared to PBMC, where it was negligible, as previously reported (21).

We also stained Tconv cells for CD101 to evaluate the frequency of CD101$^+$ Tconv cells as another indication of the tissue residency signature. We found that CD101$^+$ Tconv cells were significantly increased in the VT from BV+ compared to BV- individuals (median frequency 27% BV- vs 38% BV+, p_{adj} = 0.0118; **Table S3.7**) in contrast to the CX and PBMC (**Fig 4d**). CD101$^+$ Tconv frequency was also higher in the VT and CX compared to the PBMC regardless of BV status, supporting a role for CD101 in mediating tissue localization (**Fig 4d**). These data suggest that BV promotes tissue-resident Tconv phenotypes in the VT of BV+ individuals.

Th17 cells display increased markers of tissue residency in VT samples from individuals with BV

Lineage-specific Th17 Tconv (Th17) cells have been shown to play a role in immune responses to extracellular bacteria (57-59). To investigate the role that vaginal bacterial dysbiosis has on Th17 cell modulation, we first analyzed the frequency of Th17 cells (defined as $CD161^{+}CCR6^{+}$ Tconv cells (60)) among total Tconv cells and found that BV+ individuals did not have increased frequency of this phenotype in any of the tissue types compared to BV- individuals (**Fig 5a**). However, when we evaluated Th17 cells for specific phenotypes, we found that the frequency of tissue-resident ($CD69^{+}CD103^{+}$ expressing) Th17 cells among total Th17 cells was significantly increased in the VT of BV+ compared to BV- individuals (median 49% BV- vs 59% BV+, $p_{adj} = 0.0059$, **Table S3.7**) (**Fig 5b**). In addition, the frequency of Th17 cells expressing CD101 was also significantly increased in the VT of BV+ compared to BV- individuals (median 47% BV- vs 65% BV+, $p_{adj} = 0.0024$, **Table S3.7**) (**Fig 5c**). The frequency of Th17 cells expressing the activation marker and HIV co-receptor CCR5 was not significantly different between BV- vs BV+ individuals, although notably, the median frequency of Th17 cells expressing CCR5 in the VT of BV+ individuals was 97% (**Table S3.7**) (**Fig 5d**). Therefore, Th17 cells almost invariably express the HIV coreceptor, CCR5, coinciding with previous reports that Th17 cells are viable targets for HIV transmission (61). These results demonstrate that BV driven increased tissue-resident or CD101-expressing VT Th17 cells may present another mechanism for increased HIV susceptibility in individuals with BV.

Regulatory T cells may inhibit immune activation in the VT of individuals with BV

Regulatory T cells (Tregs) contribute to the homeostasis of the immune environment by suppressing immune activation (62). To further investigate inhibitory mechanisms associated with immune dysfunction, we characterized Tregs ($CD3^{+}CD4^{+}CD25^{+}CD127^{low}Foxp3^{+}$, **Fig S1)**

in individuals with or without BV (**Table S3.10-12**). Treg frequency among all $CD45^+$ cells was not significantly different between BV- vs BV+ in any of the tissues examined (**Fig 6a**). Upon evaluation of Treg phenotypes, we found a significant increase in $CXCR3^+$ Tregs in VT samples from BV+ compared to BV- individuals (median frequency 32% BV- vs 74% BV+, p_{adj} = 0.0039, **Table S3.10**), with no differences observed in CX or PBMC samples (**Fig 6b**). CXCR3 is associated with recruitment via chemokine signaling and activation (63) that may contribute to increased suppressive function of Tregs. We also analyzed Tregs for phenotypes differentially expressed in the VT Tconv population of BV+ individuals. We observed no significant differences in $CD69^+CD103^+$ Treg or $CD101^+$ Treg frequency in VT, CX, or PBMC samples from BV- vs BV+ individuals (**Figs 6c-d**), nor any significant differences in other activation markers examined in the VT of BV- vs BV+ individuals (**Table S3.10**).

BV promotes the expression of cytokines and chemokines in the CVT

To investigate the soluble immune factors associated with individuals with BV versus those without BV, we analyzed 71 cytokines and chemokines in serum and CVT fluid collected via menstrual cup. In the menstrual cup fluid, 61 different cytokines and chemokines met the criteria for continuous analysis, while 10 cytokines and chemokines were analyzed as a dichotomous outcome (detected/not detected). In the serum, 52 different cytokines and chemokines met the criteria for continuous analysis, 17 cytokines and chemokines were analyzed using the dichotomous outcome, and 2 cytokines were detectable in all individuals but had greater than 20% of samples out of range high so were excluded from the analysis (**Table S4**). We observed significantly higher concentrations of Leukemia Inhibitory Factor (LIF), IL-23, IL-12p70, M-CSF, and Eotaxin in the menstrual cup fluid collected from participants with versus

without BV (**Fig 7a**). Additionally, we observed significantly lower concentrations of CXCL9 and thymus and activation regulatory chemokine (TARC) (**Fig 7a**) in participants with BV versus those without BV. In our analysis of serum cytokines, we observed no significant differences in quantifiable cytokines (**Fig 7b**). For cytokines that did not meet the criteria for quantitative analyses, SDF-1α/β was detected significantly more frequently in menstrual cup fluid collected from BV- vs BV+ participants (**Fig 7c**). While we observed significantly greater concentrations of IL-12p70 in cervicovaginal fluid from BV+ individuals, we observed a significantly lower proportion of detection of serum IL-12p70 in the presence versus absence of BV (**Fig 7d**), suggesting a distinct role for IL-12p70 in the CVT immune environment compared to circulation. Overall, differentially expressed cytokines were primarily observed in menstrual cup samples, as opposed to serum samples, highlighting that BV has the greatest effects on the local CVT immune environment.

Discussion

A critical fact underlying the HIV pandemic is that T cells serve as a double-edged sword: acting as targets for HIV infection and replication, while also mediating anti-viral functions required to fight the virus (64, 65). The findings presented here suggest that previous explanations for the observed increased risk of HIV infection in the context of BV may have focused too heavily on the target cell side of that sword without appreciating BV's impact on altering T cell functionality.

In contrast to prior studies that identified increased $CD3^+CD4^+CCR5^+$ HIV target cells in samples from the CVT lumen (7, 39, 40), our analysis of tissue sections revealed that $CD3^+CD4^+CCR5^+$ HIV target cells are significantly reduced in the VT lamina propria of BV+ individuals. This seeming contradiction may be explained by the recognition that our tissue samples capture changes in cell constituents of the vaginal lamina propria that would be missed by sampling only the CVT lumen. Our results underscore that the abundance of $CD3^+CD4^+CCR5^+$ HIV target cells within VT tissues may not be the primary mechanism for the observed increase in HIV susceptibility in the context of BV. Our application of high-parameter, high-throughput flow cytometry on cells isolated from VT and CX tissue biopsies as well as PBMCs documents that BV may alter T cell functionality in the VT mucosa in addition to identifying alternate HIV target cells that may be relevant for HIV susceptibility.

We observed an increased frequency of $CD4^+$ Tconv cells expressing CD39 in the VT of BV+ individuals. The potential dysfunction of this T cell phenotype is suggested by prior studies showing $CD39^+$ T cells have a decreased response to vaccines and an increased likelihood of undergoing apoptosis (49), raising the possibility that in the context of BV, VT $CD4^+$ Tconv may exhibit increased intrinsic immunoregulation leading to reduced effector potential. This could

lead to increased HIV susceptibility through an inability to mount an effective anti-viral response upon exposure to the virus.

We also observe a significant reduction of TCF-1$^+$ CD4$^+$ Tconv in the VT of BV+ individuals (**Fig 4b**). TCF-1 is necessary for follicular T cell differentiation (50-52) and has been shown to play a role in Th17 responses by inhibiting IL-17 production (55). Fewer progenitor CD4$^+$ T cells implies that more T cells are terminally differentiated in the VT which may limit lineage-specific differentiation upon secondary exposure.

We also found that CD101$^+$ Tconv cells, and specifically CD101$^+$ Th17 cells, are more frequently observed in the VT of BV+ individuals (**Fig 4d, Fig 5c**). Less is known about the function of CD101$^+$ T cells in comparison to the other phenotypes analyzed in this study, but CD101$^+$ T cells have been associated with decreased expansion after adoptive transfer in mice (66), suggesting CD101$^+$ Tconv cells are inhibited and less likely to undergo proliferation. Additionally, CD101 is associated with exhausted T cell phenotypes that result from chronic activation and can promote immune dysfunction (67-69). Thus, the increased abundance of CD101$^+$ Tconvs and Th17 cells in the VT of BV+ individuals may also contribute to a dysfunctional Tconv immune response upon secondary exposure to HIV in the VT of BV+ individuals. Given the often recurrent and persistent nature of BV (44), chronic immune activation from repeated antigen exposure caused by BV-associated microbiota may lead to the progression of these observed dysfunctional phenotypes that could promote HIV susceptibility by limiting antiviral T cell function, expansion, and differentiation.

In addition to CD4$^+$ T cells expressing CCR5, it has been shown that CD69$^+$CD4$^+$ T cells are associated with increased susceptibility to HIV infection in the CVT mucosal tissue (70). This suggests that the enrichment of T_{RM} in the VT of BV+ individuals may mediate increased

HIV acquisition in the context of BV. In particular, the enriched Th17 T_{RM} population of the VT (**Fig 5b**), which highly expresses CCR5, provide a suitable target for HIV acquisition in BV+ individuals, consistent with previous reports that Th17 cells serve as primary target cells during vaginal SIV infection (71). In addition to the role $CD4^+$ T_{RM} in CVT mucosa play in HIV infection, they also act as reservoirs for HIV viral replication which can occur during early HIV infection (72). The increased frequency of Tconv T_{RM}, and in particular Th17 T_{RM}, may not just greatly contribute to susceptibility to primary HIV infection, but may also promote viral replication in the VT of BV+ individuals.

Further supporting the hypothesis that Th17 cells play a role in BV-associated immune modulations, our cytokine analysis revealed significant increases in IL-23, IL-12p70, M-CSF, and LIF collected in CVT fluid samples from BV+ individuals (**Fig 7a**). IL-23 and IL-12p70 can affect a variety of pro-inflammatory responses, one being the enhancement of Th17-mediated inflammation (73, 74). IL-23 and IL-12p70 may activate Th17 responses in the context of BV. The activation of Th17 cells may then lead to the formation of Th17 T_{RM}. Additionally, M-CSF, produced by macrophages, has been shown to promote Th17 differentiation of $CD4^+$ memory T cells (75), which may also contribute to the expanded Th17 T_{RM} pool in the VT of BV+ individuals. LIF, on the other hand, inhibits inflammatory responses including Th17-mediated immune responses (76). LIF may be produced in response to the activation of Th17 cell responses to limit overall Th17 cell differentiation. The reduction of TCF-1^+ progenitor Tconv cells and the production of LIF in the VT could limit the differentiation of progenitor T cells to Th17 cells which could explain why we observe comparable frequencies of total Th17 cells in individuals with or without BV.

While $CD8^+$ T cells were observed more frequently in the VT of BV+ individuals (**Fig 2c**), we only found one phenotypic difference in these cells that was associated with BV: a reduction in HLA-DR^+CD38^+ $CD8^+$ T cells (**Fig 3a**). This suggests that although VT $CD8^+$ T cells are abundant during BV, they are not overly active. Activated $CD8^+$ T cells are thought to play a role in controlling HIV after infection (77, 78). The inhibition of $CD8^+$ T cell activation observed in individuals with BV may relate to increased Tconv dysfunction, as $CD4^+$ Tconv cells are known to enhance $CD8^+$ T cell effector function (79). The interactions, or possibly lack thereof, between $CD8^+$ T cells and dysfunctional Tconv cells in the context of BV, may thus also impact $CD8^+$ T cell activation after HIV exposure and contribute towards increased HIV susceptibility in BV+ individuals.

In addition to the inhibitory function observed on Tconv cells, Tregs serve to extrinsically restrain T cell responses via active suppressive mechanisms. Expression of the chemokine receptor and activation marker CXCR3 is increased on VT Tregs in BV+ individuals. CXCR3 plays a role in T cell trafficking and is activated by the chemokines CXCL9 (MIG), CXCL10 (IP-10), and CXCL11 (I-TAC) (63). In our CVT fluid cytokine analysis, we observed a significant reduction of one of the ligands for CXCR3, CXCL9 (**Figure 7a**), as well as a trend towards lower concentrations of CXCL10. While other studies have also reported a reduction in local CXCL9 and CXCL10 in the CVT in BV+ individuals (19, 80-82), it is unclear how to interpret this reduction in chemokine ligands along with our finding that their CXCR3 chemokine receptor is increased on Tregs. One possible explanation is that chemokine production within the deeper tissue compartment that may be involved in recruiting cells expressing CXCR3 may not be captured in the CVT lumen. Nonetheless, activated $CXCR3^+$

Tregs in the VT may inhibit immune activation and contribute to dysregulated phenotypes observed in the VT of BV+ individuals.

In our chemokine analysis, we observed a significant reduction of TARC in CVT fluid samples from BV+ individuals (**Fig 7a**). TARC has been associated with the recruitment of Th2 cells (83, 84), which also rely on TCF-1 to promote Th2 differentiation and regulation of function (54). Th2 cells are typically associated with allergic and anti-parasitic responses (85) and have been rarely studied in the CVT. While they are not thought to contribute a significant role in BV associated immune responses, the reduction of TCF-1 and TARC in BV+ individuals does suggest that Th2-specific responses may be reduced in the context of BV. The significantly increased expression of Eotaxin that we identified in CVT fluid samples of BV+ individuals (**Fig 7a**) may arise to compensate for reduced Th2-specific responses that recruit eosinophils (86). Eotaxin is primarily produced by epithelial and endothelial cells and enhances the recruitment of eosinophils (87). Eosinophils are also not typically involved in bacterial-specific immune responses and this likely has little impact on HIV susceptibility but this does further support the notion that T cell mechanisms are more dysfunctional in BV+ individuals.

In our CVT fluid cytokine analysis, we also observed increased detection of SDF-1α/β in BV+ individuals (**Fig 7c**). As a natural ligand for CXCR4, an HIV coreceptor (88-90), increased SDF-1α/β expression might be expected to increase HIV resistance by decreasing CXCR4 expression. Therefore, if SDF-1α/β plays a role in promoting HIV susceptibility in individuals with BV, the mechanism for this is unclear. Finally, we observed no significant difference in IL-1β in CVT samples from BV+ vs BV- individuals. Although IL-1β is frequently identified as increased in CVT fluid with BV, this is not a universal observation (91, 92). The factors that mediate altered expression of soluble immune mediators during BV have not been elucidated.

Our study had limitations: first, we focused on characterizing diverse T cell markers and a large panel of soluble immune mediators in the context of BV infection, leaving the relationship of BV with other components of the immune response unevaluated. One justification for limiting our evaluation to characteristics of $CD3^+$ T cells is that these constitute the predominant lymphocyte population in the CVT mucosa (**Fig 2a**). A second limitation was that we collected 3-mm tissue biopsies that often captured low amounts of rare T cell subsets such as Tregs. This reduced our power to evaluate the role of such subsets in immune responses to BV. A final limitation of our analysis is that it was performed as an exploratory, hypothesis-generating analysis, and as such, used nominal P values adjusted for confounders but not discounted for multiple comparisons (138 immune cell subsets comparisons, and 71 soluble mediators comparisons). Thus, our findings should be confirmed through studies employing hypothesis-driven testing.

In summary, our study performed the most comprehensive evaluation to date of CVT tissue T cell subsets associated with BV. This data shows BV driven immune alterations have the most profound impact on the VT T cells and changes at this site may be most responsible for increased HIV susceptibility in BV+ individuals. Specifically, we identify dysfunctional T cell subsets including $CD39^+$ Tconv and decreased progenitor TCF-1^+ Tconv in the VT of BV+ individuals that could alter host response and contribute to increased HIV susceptibility by limiting the antiviral capabilities of VT T cells. Furthermore, we found the enrichment of Tconv T_{RM}, and specifically the Th17 T_{RM} subset, in the VT of BV+ individuals that may serve as targets for HIV infection and replication. Confirmation of these findings and elaboration on molecular mechanisms may identify novel immune interventions to reduce the risk of adverse outcomes associated with BV, including increased risk of HIV infection.

Methods

Participants, samples, and data collection

Samples and data for this analysis came from the Kinga Study (Clinicaltrials.gov ID# NCT03701802) which enrolled a total of 406 heterosexual Kenyan couples from Oct. 2018 through Dec. 2019 to evaluate how exposure to sexually transmitted infectious agents alters genital mucosal immune responses. Among these couples, 110 were HIV serodifferent (defined as a person living with HIV (PLWH) and their heterosexual HIV-exposed partner), with the remaining 298 couples involving partners who were both HIV-seronegative at enrollment. HIV serodifferent couples were excluded if, prior to enrollment, the PLWH had initiated antiretroviral therapy (ART) with resulting suppressed HIV viral load, or the HIV-exposed partner had initiated tenofovir-based pre-exposure prophylaxis (PrEP). ART and PrEP were provided to enrolled PLWH or HIV-exposed partners, respectively, upon enrollment.

Seven sample types were requested from all Kinga Study participants at enrollment and 6-month follow-up visits for evaluation of immune responses: cervicovaginal fluid via Softcup® (menstrual cup); two 3-mm vaginal tissue biopsies with one cryopreserved for immunofluorescent imaging, and one cryopreserved for flow cytometry; two 3-mm ectocervical tissue biopsies processed in parallel to the vaginal biopsies; fractionated peripheral blood mononuclear cells; and serum were all collected (Note: genital samples and CVT fluid collection were deferred if participants were actively menstruating and participants were encouraged to return to clinic when not menstruating for collection of all sample types at the same timepoint). Swabs for BV testing were collected prior to biopsies, and BV was assessed by Nugent score with 0-3 defined as normal flora, 4-6 as intermediate flora, and 7-10 classified as BV (93). Additional demographic, epidemiologic, clinical, and sexual behavior data (including self-

reported frequency of vaginal sex, condom use, and hormonal contraceptive use) were collected at all visits.

Laboratory testing at the enrollment and 6-month follow-up visits included HIV serology by Determine HIV 1/2 Rapid diagnostic Test (RDT) (Abbott Laboratories, Inc., Abbott Park, IL, USA) with confirmation of positive results with First Response RDT (Premier Medical Corporation Ltd., Kachigam, India), and further confirmation of RDT results using 4th generation HIV-1-2 Ag/Ab Murex EIA assay (DiaSorin, Inc., Kent, UK). Herpes simplex virus type 2 (HSV-2) serology was performed with HerpeSelect 2 ELISA IgG test (Focus Technologies, Inc., Cypress, CA) using an index value cut-off of ≥3.5 to improve test specificity (94-98).

To identify samples for the current cross-sectional analysis of the effects of BV on immune responses we focused on 245 participants living without HIV who were identified as female at birth. These consisted of all 44 participants who may have been exposed to HIV by their enrolled heterosexual sexual partners, and 201 whose enrolled heterosexual sexual partner was without HIV and whose data could support a variety of analyses, including the analysis of BV mediated immune responses. Immunofluorescent imaging was performed on enrollment samples from a subset who were HSV-2 seronegative; had HIV-uninfected partners; and if the participant was BV- by Nugent score, were also BV- by Amsel criteria (99) to prioritize clean comparison groups. All immunologic testing was performed blinded to participant exposure data.

Analysis of tissue samples by immunofluorescent microscopy

Sample collection: Biopsies were collected using baby Tischler forceps at the lateral vaginal wall and the ectocervical os, embedded in optimal cutting temperature (OCT) compound and cryopreserved on dry ice.

Laboratory Analysis: Fresh frozen tissue biopsies in OCT compound were sectioned 8 µm thick using a cryostat and placed onto frosted microscope slides. Serial sections were used for hematoxylin and eosin (H&E) staining and immunofluorescent (IF) staining. H&E stained slides were used to identify lamina propria and epithelium and to evaluate tissue integrity to ensure tissue sections met the criteria for analysis (intact lamina propria and epithelium).

Tissue sections for IF staining were fixed in acetone at -20°C for five minutes, dried for thirty minutes at room temperature, and rehydrated in tris-buffered saline with 0.05% tween (TBST). Slides were quenched using 3% H_2O_2 for twenty minutes at room temperature, rinsed with TBST, and endogenous binding sites were blocked using 1:10 fish gelatin blocking agent (Biotium, Cat# 22010) diluted in TBST for one hour. Unconjugated mouse anti-human CCR5 antibody (clone MC-5 (100) provided by M. Mack) at optimal dilution (0.3 µg/ml) was added for one hour, washed with TBST, and then goat anti-mouse antibody conjugated with horseradish peroxidase (polyclonal, Invitrogen, Cat# B40961) was added for thirty minutes. After washing with TBST, a solution of Tris Buffer (100mM, MilliporeSigma, Cat# 648315), optimally diluted tyramide (AF488, Invitrogen, Cat# B40953, diluted 1:100), and H2O2 (diluted 1:67,000) was then used for immunofluorescence and signal amplification. Slides were washed with TBST and a combination of optimally diluted, directly conjugated anti-CD3 (AF594, Clone UCHT1, R&D Systems, Cat# FAB100T, diluted 1:50) and anti-CD4 (AF647, Clone RPA-T4, BioLegend, Cat# 300520, diluted 1:25) antibodies were added for incubation overnight in the 4°C fridge. Slides were then rinsed in TBST and stained with DAPI (Invitrogen, Cat# D1306, diluted 2.5 ng/ml) for

five minutes. Slides were washed with PBS, saturated briefly for ten seconds in ammonium acetate, saturated for ten minutes in copper sulfate, and then saturated again briefly for ten seconds in ammonium acetate. Slides were thoroughly rinsed in dH_2O, dried, mounted with Prolong Gold (Invitrogen, Cat# P36930) and a cover slip, and allowed to set for 24 hours.

Tissue sections were imaged within 48 hours of staining using a 20x/0.8 Pan-APOCHROOMAT air objective on a Zeiss Axio Imager Z2 microscope as part of a TissueFAXS system (TissueGnostics; Vienna, Austria) equipped with an X-cite 120Q lamp (Excelitas), and with DAPI (49000 ET), EGFP (49002 ET), Texas Red (49008 ET), and Cy5 (490006 ET) filter sets. Images were acquired using an Orca-Flash 4.0 camera (Hamamatsu) with TissueFAXS 7.1 software (TissueGnostics).

Tissue section image analysis

We quantified the density of $CD3^+$, $CD3^+CD4^+$, and $CD3^+CD4^+CCR5^+$ cells in the epithelium and lamina propria of CX and VT sections from individuals with or without BV. Images acquired using the TissueFAXS system were exported as multi-channel 16-bit tiff files of stitched regions. Cell segmentation, region of interest (ROI) selection (lamina propria vs epithelium), marker intensity thresholding, and statistical analyses were performed with a custom graphical user interface (GUI) developed in MATLAB (R2022b). Nucleus segmentation was performed by finding the regional maxima of the grayscale DAPI signal, followed by morphological thickening constrained by the binary DAPI mask. Threshold intensities for the markers of interest were set manually through the GUI. The boundary between the lamina propria and epithelium regions was segmented based on nuclear density, and further adjusted manually through the GUI. Finally, for each region (lamina propria and epithelium), the number

of single-, double-, and triple-positive cells, as well as the density (number of cells per mm^2) were extracted. Codes and an extended description of the GUI can be found at github.com/FredHutch/Kinga_Study_BV_MacLean.

Analysis of tissue samples by high-parameter flow cytometry*:*

Sample collection: Biopsies were collected using baby Tischler forceps biopsies either at the lateral vaginal wall or the ectocervical os, placed in a cryovial containing fetal bovine serum at 4^oC, and transported to the lab. In the lab, dimethyl sulfoxide (DMSO) was added to the cryovial to a final concentration of 10%, cryopreserved overnight at -80^oC, and transferred to liquid nitrogen for long-term storage.

Peripheral blood mononuclear cells (PBMCs) were isolated from acid-citrate dextrose (ACD) whole blood by centrifugation and resuspension in Dulbecco's Phosphate Buffered Saline (DPBS). Cells were centrifuged over Ficoll-Histopaque (Sigma-Aldrich, Cat# 10771) at room temperature. The buffy coat was collected and washed twice in DPBS at 4^oC before live cells were counted on a hemacytometer with trypan blue. Cells were pelleted and resuspended in 10% DMSO in fetal calf serum at 4^oC at a concentration of either 5-7 x 10^6 cells/mL, or 10-15 x 10^6 cells/mL. Cryovials with 1 mL of these PBMC suspensions were placed in controlled rate freezing equipment (Mr. Frosty) and stored overnight at -80° C. Cells were subsequently transferred to liquid nitrogen for long term storage and shipped in liquid nitrogen dry shippers to University of Washington for further analysis.

Tissue Processing for Flow Cytometry: Cryopreserved PBMCs, ectocervical biopsies, or vaginal biopsies in liquid nitrogen were quickly thawed and transferred to 10% FBS (PBMCs) or 7.5% FBS (VT/CX biopsies) complete RPMI media (RP10 or RP7.5). PBMCs were spun down and resuspended in RP10. After sitting in warmed RP7.5 for 10 minutes, biopsies were incubated

at 37 degrees C for 30 minutes with Collagenase II (Sigma-Aldrich, 700 U/mL) and DNase I (Sigma-Aldrich, 400U/mL) in RP7.5. Biopsies were then passed through a 100-mm cell strainer using a plunger to disrupt the tissue, washed, and resuspended in phosphate-buffered saline (PBS). PBMCs and cells isolated from tissues were stained immediately after processing for flow cytometry. Cryopreserved PBMCs from a healthy control donor (Seattle Area Control Cohort (SAC)) were used as a longitudinal technical control for all flow cytometry acquisitions (data not shown).

Flow Cytometry: Immediately following isolation, cells were incubated with UV Blue Live/Dead reagent (**Table S1**) in PBS for 30 mins at room temperature. After washing, cells were then stained with biotinylated CXCR3 (**Table S1**) in 0.5% FACS buffer for 20 mins at room temperature. Cells were washed and then stained extracellularly with antibodies (**Table S1**) diluted in 0.5% FACS buffer and brilliant staining buffer (BD Biosciences, Cat# 563794) for 20 mins at room temp. Cells were fixed with Foxp3 Transcription Factor Fixation/Permeabilization buffer (ThermoFisher, Cat# 00-5521-00) for 30 mins at room temp. Cells were washed and then stained intracellularly with antibodies diluted in 1X Permeabilization Buffer (ThermoFisher, Cat# 00-8333-56) for 30 mins at room temp. Cells were then resuspended in 200 ml 0.5% FACS buffer and stored at 4 degrees until ready for use. Antibodies were titrated and used at optimal dilution. Staining was performed in 5-ml polystyrene tubes (Falcon, Cat# 352054). Analysis was performed using Flowjo software and we required at least 25 cells for analysis of phenotypes associated with the parent cell type and further downstream gating and analysis (**Fig S1**).

Cytokine and chemokine sample collection, and processing

Cervicovaginal fluid: The menstrual cup was inserted into the vaginal canal beneath the cervix at the beginning of the study visit and remained in place for a minimum of 15 and a maximum of 60 minutes while other visit procedures were being conducted. Sample collection was deferred if the participant was menstruating. The participant was encouraged to move around while the menstrual cup was in place. Once removed, the menstrual cup and all CVT fluid contents were placed in a 50 mL sterile collection tube and transported to the lab on ice. CVT fluids were collected in the 50 mL collection tube by centrifuging at 1500 rpm (320xg) for 10 min at 4°C. The mucous and fluids were gently mixed and 200-300 µl was aliquoted with a 1000 mL pipet tip into each cryovial and stored at -80°C.

Serum: Whole blood was collected in an SST vacutainer, allowed to clot for less than 2 hours, and centrifuged at 1300g for 15 minutes. Serum was aliquoted and stored at -80°C.

Soluble mediator assays: Serum and menstrual cup (CVT fluid) aliquots were shipped on dry ice to Eve Technologies (Calgary, Alberta, Canada). All samples were measured upon the first thaw. CVT fluid samples were weighed and diluted in PBS at a ratio of 1g sample to 1mL PBS. CVT fluid samples were vortexed for 2 minutes and up to 500 µl was loaded into 0.2 µm low-bind spin filters (MilliporeSigma, Cat# CWLS01S03) and centrifuged at ~14,000 x g for 15 mins to remove the mucus from the samples prior to analysis. Levels of cytokines and chemokines from CVT fluid and serum samples were measured using the Human Cytokine Array/Chemokine Array 71-403 Plex Panel (Eve Technologies, HD71).

Statistics

For purposes of data analysis, BV+ was defined by Nugent score of 7-10. BV- was defined as normal flora by Nugent score 0-3. For flow cytometry and soluble mediator analyses,

to maximize the size of our BV+ group, we used enrollment visits of participants who were BV+ at enrollment, augmented with the six-month visit from any additional participants who were BV+ at the six-month exit visit. Thus, our BV+ group consisted of one time point per individual, but in some cases, it was enrollment while for others it was at exit. Among the remaining individuals, enrollment visits from those with normal flora at enrollment served as the BV- reference group. For immunofluorescent imaging, all specimens were from enrollment.

Cell densities of $CD3^+$, $CD3^+CD4^+$, and $CD3^+CD4^+CCR5^+$ cells in tissue sections were compared between individuals with versus without BV using the Wilcoxon rank sum test. To estimate adjusted differences in the percentage of T-cells with specified markers from flow cytometry data by BV status, we used rank-based regression, a nonparametric method robust to outliers (101). To investigate associations of soluble mediators in serum and CVT fluid samples with BV status, we first determined whether, for each mediator, at least 80% of the specimens generated a quantifiable level (vs out of quantifiable range or missing for another reason). If at least 80% of results were quantifiable, we imputed out of range values by randomly selecting a value between the lowest observed value and half the lowest observed value (if out of range low), or by selecting the largest observed value (if out of range high). We then compared $\log_{10}$-transformed levels of the mediator from individuals in BV+ vs BV- groups using a t-test and estimated differences in mean log cytokine concentrations from both serum and CVT fluid samples using linear regression. If <80% of the levels for a mediator were quantifiable, we categorized the mediator as detected vs not detected and estimated the odds ratio for the effect of BV on mediator detection using logistic regression. For both flow cytometry and soluble mediator data, results from VT and CX samples were adjusted for hormonal contraceptive use (yes, no and menstruating, no and amenorrheal), HSV-2 serology (positive, negative,

indeterminate), HIV exposure (HIV status of sexual partner), and number of unprotected sex acts in the last thirty days (continuous), while results from PBMC samples were adjusted for hormonal contraceptive use (yes, no and menstruating, no and amenorrheal), only. In this exploratory work, we did not adjust p-values for multiple testing. Statistical analyses were conducted using R version 4.3.3.

Study approval

All participants provided written informed consent using documents reviewed and approved by the University of Washington institutional review board, and the Scientific and Ethics Review Unit of the Kenya Medical Research Institute.

Data availability

All supporting data are included in the supplemental figures and tables.

Author contributions:

FM, JBG, JLS, SCV, NP, ICT, and LW conducted the experiments. FM, ATT, JLS, CM, and KKT analyzed data, MM provided reagents, JD and LKS contributed analysis methods, BHC, KN, NM, JRL, and JML designed the research study, and FM, MCS, JRL, and JML wrote the first draft of the manuscript. All authors edited and approved the manuscript.

Acknowledgements:

We thank all study volunteers for their participation in the Kinga Study and their willingness to provide many different samples. Additionally, we thank the members of the Kinga Study team and the Lund and Prlic labs for their helpful discussions on experimental findings and manuscript preparation throughout this process. Additionally, we would like to thank the Fred Hutchinson Cancer Center Cellular Imaging Shared Resource, supported by the Fred Hutchinson Cancer Center Cellular Imaging Core Facility (RRID:SCR_022609) of the Fred Hutch/University of Washington/Seattle Children's Cancer Consortium (P30 CA015704), for assistance with microscopy and image analysis. This work was supported by the following grants from the National Institutes of Health: R01 AI131914 (to J.M.L and J.R.L.), R01 AI141435 (to J.M.L.), and R01 AI129715 (to J.R.L). S.V. was supported by T32 AI007509, I.C.T. was supported by T32 AI007140 and L.W. was supported by T32 AI083203.

Kinga Study Team:

University of Washington: International Clinical Research Center

Jairam R Lingappa (co-Principal Investigator and Protocol Chair), Justice Quame-Amaglo (study coordinator), Harald Haugen, Elena Rechkina, Daphne Hamilton, Matthew Ikuma, Marie Bauer, Xuanlin Hou, Zarna Marfatia, Katherine Thomas, Corinne Mar, Adino Tesfahun Tsegaye

Fred Hutchinson Cancer Center:

Jennifer Lund (co-Principal Investigator), Jessica Graham, Jessica Swarts, Sarah Vick, Nicole Potchen, Irene Cruz Talevara, Lakshmi Warrier, Finn MacLean, Elizabeth McCarthy

Kenya Medical Research Institute: Thika Partners in Health Research and Development (and Jomo Kenyatta University [JKUAT])

Nelly R. Mugo (Site Principal Investigator), Kenneth Ngure (Site Investigator), Catherine Kiptinness (site coordinator), Bhavna H. Chohan (Site Laboratory Director), Nina Akelo, Charlene Biwott, Stephen Gakuo, Elizabeth Irungu, Marion Kiguoya, Edith Kimani, Eric Koome, Solomon Maina, Linet Makena, Sarah Mbaire, Murugi Micheni, Peter Michira, Jacinta Nyokabi, Peter Mogere, Richard Momanyi, Edwin Mugo, Caroline Senoga, Mary Kibatha, Jelioth Muthoni, Euticus Mwangi, Philip Mwangi, Margaret Mwangi, Charles Mwangi, Stanley Mugambi Ndwiga, Peter Mwenda, Grace Ndung'u, Faith Njagi, Zakaria Njau, Irene Njeru, John Njoroge, Esther Njoroge, John Okumu, Lynda Oluoch, Judith Achieng Omungo.

Figure Legends

Figure 1. BV is associated with a decreased abundance of $CD3^+CD4^+CCR5^+$ cells in the VT lamina propria. (a) Representative hematoxylin and eosin-stained vaginal tract tissue section imaged with brightfield microscopy. (b) Representative immunofluorescent stained tissue section from the same vaginal tract (VT) biopsy as Figure 1a. DAPI stain is shown in blue, the CD3 stain is shown in red, the CD4 stain is shown in cyan, and the CCR5 stain is shown in green. All fluorescent signals overlayed. (c-f) Comparison of the cell density of CD3+ T cells, CD3+/CD4+ T cells or CD3+/CD4+/CD5+ HIV target cells between BV negative and BV positive samples in the VT Lamina Propria (c), VT Epithelium (d), CX Lamina Propria (e) and CX Epithelium (f). Wilcoxon T-test was performed for each comparison shown. "ns" labeled comparisons are not significant with $p > 0.05$.

Figure 2. $CD8^+$ T cell abundance increases in the VT tissues of individuals with BV. Flow cytometry was used to quantify the proportions of T cells within different tissue sites as indicated. (a) The frequency of $CD3^+$ among the total $CD45^+$ population in ectocervix (CX), vaginal tract (VT), and peripheral mononuclear blood cells (PBMC) samples in BV- and BV+ individuals. The frequency of Tconv ($CD3^+CD4^+CD25^-$ cells) (b) and $CD3^+CD8^+$ (c) among the total $CD45^+$ population in CX, VT, and PBMC samples in BV- and BV+ individuals. The frequency of Tconv (d) and $CD8^+$ (e) among the total $CD3^+$ population in CX, VT, and PBMC samples in BV- and BV+ individuals. Adjusted rank regression T test performed to compare frequencies in each tissue between BV- and BV+ individuals. Adjusted p-value displayed when $p \leq 0.05$, and the p-value is labeled “ns” for not significant when adjusted $p > 0.05$.

Figure 3. Few phenotypic alterations in CVT or circulating $CD8^+$ T cells in individuals with BV. Flow cytometry was used to examine $CD8^+$ T cell phenotypes within different tissue sites as indicated. The frequency of HLA-DR^+CD38^+ (a), Granzyme B^+ (b), $CD69^+CD103^+$ (c), and $CD101^+$ (d) among the total $CD8^+$ T cell population in CX, VT, and PBMC samples in BV- and BV+ individuals. Adjusted rank regression T test performed to compare frequencies in each tissue between BV- and BV+ individuals. Adjusted p-value displayed when $p \leq 0.05$, and the p-value is labeled "ns" for not significant when adjusted $p > 0.05$.

Figure 4. BV is associated with an increase in Tconv with reduced functional potential as well as an increase in the fraction of Tconv with a T_{RM} phenotype in the VT. Flow cytometry was used to examine Tconv cell phenotypes within different tissue sites as indicated. (a) The frequency of $CD39^+$ (a), T cell factor 1 (TCF-1^+) (b), $CD69^+CD103^+$ (c), and $CD101^+$ (d) among the total Tconv T cell population in CX, VT, and PBMC samples in BV- and BV+ individuals. Adjusted rank regression T test performed to compare frequencies in each tissue between BV- and BV+ individuals. Adjusted p-value displayed when $p \leq 0.05$, and the p-value is labeled "ns" for not significant when adjusted $p > 0.05$.

Figure 5. Increased fractions of VT Th17 cells have a T_{RM} phenotype in individuals with BV. Flow cytometry was used to examine Th17 cell phenotypes within different tissue sites as indicated. (a) The frequency of Th17 T cells, defined as $CD161^+CCR6^+$ Tconv, among the total Tconv T cell population in CX, VT, and PBMC samples in BV- and BV+ individuals. (b) The frequency of $CD69^+CD103^+$ (b), $CD101^+$ (c), and $CCR5^+$ (d) among the total Th17 T cell

population in CX, VT, and PBMC samples in BV- and BV+ individuals. Adjusted rank regression T test performed to compare frequencies in each tissue between BV- and BV+ individuals. Adjusted p-value displayed when $p \leq 0.05$, and the p-value is labeled "ns" for not significant when adjusted $p > 0.05$.

Figure 6. Regulatory T cell expression of CXCR3 in the VT is associated with BV. Flow cytometry was used to examine regulatory T cell phenotypes within different tissue sites as indicated. (a) The frequency of regulatory T cells (Tregs; $CD3^{+}CD4^{+}CD25^{+}CD127^{low}Foxp3^{+}$) among the total Tconv T cell population in CX, VT, and PBMC samples in BV- and BV+ individuals. (b) The frequency of $CXCR3^{+}$ (b), $CD69^{+}CD103^{+}$ (c), $CD101^{+}$ (d) among the total Treg population in CX, VT, and PBMC samples in BV- and BV+ individuals. Adjusted rank regression T test performed to compare frequencies in each tissue between BV- and BV+ individuals. Adjusted p-value displayed when $p \leq 0.05$, and the p-value is labeled "ns" for not significant when adjusted $p > 0.05$.

Figure 7. BV drives unique cytokine production in CVT fluid. Luminex was used to quantify cytokines and chemokines from CVT fluid or serum samples. Adjusted difference (BV positive – BV negative) for CVT fluid cytokines (a) and serum (b) that met the criteria for quantification of cytokine concentrations (greater than or equal to 80% of samples were detectable). Adjusted odds ratio (BV positive/BV negative) for CVT fluid cytokines (c) and serum (d) that did not meet the criteria for quantification of cytokine concentrations (less than 80% of samples were detectable). The 95% confidence interval is shown for all comparisons. Significant results when

adjusted $p \leq 0.05$ comparing BV- vs BV+ are colored in orange and non-significant differences $p > 0.05$ comparing BV- vs BV+ are purple.

Supplementary Figure 1. Flow cytometry gating to determine phenotype expression on individual cells. Cells were gated by forward scatter height (FSC-H) and forward scatter area (FSC-A) to filter out non-singlet cells. Then cells were gated by side scatter area (SSC-A) and forward scatter area (FSC-A) to isolate lymphocytes. Lymphocytes were analyzed by live/dead and CD45 expression. Live $CD45^+$ cells were then analyzed for CD3 expression. $CD3^+$ cells were then analyzed for CD4 and CD8 expression. $CD8^+CD4^-$ were analyzed for the phenotypes listed. $CD4^+CD8^-$ were analyzed for CD25 and CD127 expression. $CD25^-$ cells were defined as conventional $CD4^+$ T cells (Tconv). $CD25^+CD127^{low}$ were analyzed for Foxp3 expression. $Foxp3^+$ among the $CD25^+CD127^{low}$ population were defined as regulatory T cells (Tregs). Tregs were analyzed for the phenotypes listed. Tconv were analyzed for the phenotypes listed. In addition, Tconv were analyzed for T-bet expression which defined Th1 cells, and $CCR6^+CD161^+$ co-expression which defined Th17 cells. Th1 and Th17 cells were also analyzed for expression of the phenotypes listed. For each gating analysis, samples were only continued for further analysis if the parent gate had a minimum of 25 cells.

Table Legends

Table 1. Demographic and clinical data from 212 participants included in this analysis.

Table S1. Antibodies used for high parameter flow cytometry on biopsies and peripheral blood mononuclear cells.

References

1. Dabee S, Passmore JS, Heffron R, and Jaspan HB. The Complex Link between the Female Genital Microbiota, Genital Infections, and Inflammation. *Infect Immun.* 2021;89(5).
2. Peebles K, Velloza J, Balkus JE, McClelland RS, and Barnabas RV. High Global Burden and Costs of Bacterial Vaginosis: A Systematic Review and Meta-Analysis. *Sex Transm Dis.* 2019;46(5):304-11.
3. Sobel JD. Vaginitis. *N Engl J Med.* 1997;337(26):1896-903.
4. Allsworth JE, Lewis VA, and Peipert JF. Viral sexually transmitted infections and bacterial vaginosis: 2001-2004 National Health and Nutrition Examination Survey data. *Sex Transm Dis.* 2008;35(9):791-6.
5. Atashili J, Poole C, Ndumbe PM, Adimora AA, and Smith JS. Bacterial vaginosis and HIV acquisition: a meta-analysis of published studies. *AIDS.* 2008;22(12):1493-501.
6. Cohen CR, Duerr A, Pruithithada N, Rugpao S, Hillier S, Garcia P, et al. Bacterial vaginosis and HIV seroprevalence among female commercial sex workers in Chiang Mai, Thailand. *AIDS.* 1995;9(9):1093-7.
7. Gosmann C, Anahtar MN, Handley SA, Farcasanu M, Abu-Ali G, Bowman BA, et al. Lactobacillus-Deficient Cervicovaginal Bacterial Communities Are Associated with Increased HIV Acquisition in Young South African Women. *Immunity.* 2017;46(1):29-37.
8. Jain JP, Bristow CC, Pines HA, Harvey-Vera A, Rangel G, Staines H, et al. Factors in the HIV risk environment associated with bacterial vaginosis among HIV-negative female

sex workers who inject drugs in the Mexico-United States border region. *BMC Public Health.* 2018;18(1):1032.

9. Massad LS, Daubert EM, Evans CT, Minkoff H, Kassaye S, Dionne-Odom J, et al. Trends in Bacterial Vaginosis Prevalence in a Cohort of U.S. Women with and at Risk for HIV. *J Womens Health (Larchmt).* 2022;31(5):726-32.

10. Sewankambo N, Gray RH, Wawer MJ, Paxton L, McNaim D, Wabwire-Mangen F, et al. HIV-1 infection associated with abnormal vaginal flora morphology and bacterial vaginosis. *Lancet.* 1997;350(9077):546-50.

11. Taha TE, Hoover DR, Dallabetta GA, Kumwenda NI, Mtimavalye LA, Yang LP, et al. Bacterial vaginosis and disturbances of vaginal flora: association with increased acquisition of HIV. *AIDS.* 1998;12(13):1699-706.

12. Hillier SL, Nugent RP, Eschenbach DA, Krohn MA, Gibbs RS, Martin DH, et al. Association between bacterial vaginosis and preterm delivery of a low-birth-weight infant. The Vaginal Infections and Prematurity Study Group. *N Engl J Med.* 1995;333(26):1737-42.

13. Hillier SL, Martius J, Krohn M, Kiviat N, Holmes KK, and Eschenbach DA. A case-control study of chorioamnionic infection and histologic chorioamnionitis in prematurity. *N Engl J Med.* 1988;319(15):972-8.

14. Watts DH, Krohn MA, Hillier SL, and Eschenbach DA. Bacterial vaginosis as a risk factor for post-cesarean endometritis. *Obstet Gynecol.* 1990;75(1):52-8.

15. Torrone EA, Morrison CS, Chen PL, Kwok C, Francis SC, Hayes RJ, et al. Prevalence of sexually transmitted infections and bacterial vaginosis among women in sub-Saharan

Africa: An individual participant data meta-analysis of 18 HIV prevention studies. *PLoS Med.* 2018;15(2):e1002511.

16. Spear GT, St John E, and Zariffard MR. Bacterial vaginosis and human immunodeficiency virus infection. *AIDS Res Ther.* 2007;4:25.

17. St John E, Mares D, and Spear GT. Bacterial vaginosis and host immunity. *Curr HIV/AIDS Rep.* 2007;4(1):22-8.

18. Cauci S, Culhane JF, Di Santolo M, and McCollum K. Among pregnant women with bacterial vaginosis, the hydrolytic enzymes sialidase and prolidase are positively associated with interleukin-1beta. *Am J Obstet Gynecol.* 2008;198(1):132 e1-7.

19. Shvartsman E, Perciani CT, Richmond MEI, Russell JNH, Tough RH, Vancuren SJ, et al. Gardnerella subgroup dominant microbiomes are associated with divergent cervicovaginal immune responses in a longitudinal cohort of Kenyan women. *Front Immunol.* 2022;13:974195.

20. Monin L, Whettlock EM, and Male V. Immune responses in the human female reproductive tract. *Immunology.* 2020;160(2):106-15.

21. Woodward Davis AS, Vick SC, Pattacini L, Voillet V, Hughes SM, Lentz GM, et al. The human memory T cell compartment changes across tissues of the female reproductive tract. *Mucosal Immunol.* 2021;14(4):862-72.

22. Pattacini L, Woodward Davis A, Czartoski J, Mair F, Presnell S, Hughes SM, et al. A pro-inflammatory CD8+ T-cell subset patrols the cervicovaginal tract. *Mucosal Immunol.* 2019;12(5):1118-29.

23. Kumar BV, Ma W, Miron M, Granot T, Guyer RS, Carpenter DJ, et al. Human Tissue-Resident Memory T Cells Are Defined by Core Transcriptional and Functional Signatures in Lymphoid and Mucosal Sites. *Cell Rep.* 2017;20(12):2921-34.

24. Cibrian D, and Sanchez-Madrid F. CD69: from activation marker to metabolic gatekeeper. *Eur J Immunol.* 2017;47(6):946-53.

25. Mackay LK, Braun A, Macleod BL, Collins N, Tebartz C, Bedoui S, et al. Cutting edge: CD69 interference with sphingosine-1-phosphate receptor function regulates peripheral T cell retention. *J Immunol.* 2015;194(5):2059-63.

26. Shiow LR, Rosen DB, Brdickova N, Xu Y, An J, Lanier LL, et al. CD69 acts downstream of interferon-alpha/beta to inhibit S1P1 and lymphocyte egress from lymphoid organs. *Nature.* 2006;440(7083):540-4.

27. Pham TH, Okada T, Matloubian M, Lo CG, and Cyster JG. S1P1 receptor signaling overrides retention mediated by G alpha i-coupled receptors to promote T cell egress. *Immunity.* 2008;28(1):122-33.

28. Keller HR, Ligons DL, Li C, Hwang S, Luckey MA, Prakhar P, et al. The molecular basis and cellular effects of distinct CD103 expression on CD4 and CD8 T cells. *Cell Mol Life Sci.* 2021;78(15):5789-805.

29. Sathaliyawala T, Kubota M, Yudanin N, Turner D, Camp P, Thome JJ, et al. Distribution and compartmentalization of human circulating and tissue-resident memory T cell subsets. *Immunity.* 2013;38(1):187-97.

30. Clark RA, Watanabe R, Teague JE, Schlapbach C, Tawa MC, Adams N, et al. Skin effector memory T cells do not recirculate and provide immune protection in alemtuzumab-treated CTCL patients. *Sci Transl Med.* 2012;4(117):117ra7.

31. Elliott Williams M, Hardnett FP, Sheth AN, Wein AN, Li ZT, Radzio-Basu J, et al. The menstrual cycle regulates migratory CD4 T-cell surveillance in the female reproductive tract via CCR5 signaling. *Mucosal Immunol.* 2024;17(1):41-53.

32. Schenkel JM, Fraser KA, Vezys V, and Masopust D. Sensing and alarm function of resident memory CD8(+) T cells. *Nat Immunol*. 2013;14(5):509-13.

33. Beura LK, Fares-Frederickson NJ, Steinert EM, Scott MC, Thompson EA, Fraser KA, et al. CD4(+) resident memory T cells dominate immunosurveillance and orchestrate local recall responses. *J Exp Med.* 2019;216(5):1214-29.

34. Schenkel JM, Fraser KA, Beura LK, Pauken KE, Vezys V, and Masopust D. T cell memory. Resident memory CD8 T cells trigger protective innate and adaptive immune responses. *Science*. 2014;346(6205):98-101.

35. Kumar BV, Connors TJ, and Farber DL. Human T Cell Development, Localization, and Function throughout Life. *Immunity*. 2018;48(2):202-13.

36. Rodriguez-Garcia M, Connors K, and Ghosh M. HIV Pathogenesis in the Human Female Reproductive Tract. *Curr HIV/AIDS Rep.* 2021;18(2):139-56.

37. Mitchell C, and Marrazzo J. Bacterial vaginosis and the cervicovaginal immune response. *Am J Reprod Immunol.* 2014;71(6):555-63.

38. Rebbapragada A, Howe K, Wachihi C, Pettengell C, Sunderji S, Huibner S, et al. Bacterial vaginosis in HIV-infected women induces reversible alterations in the cervical immune environment. *J Acquir Immune Defic Syndr*. 2008;49(5):520-2.

39. Giraldo PC, de Carvalho JB, do Amaral RL, da Silveira Goncalves AK, Eleuterio J, Jr., and Guimaraes F. Identification of immune cells by flow cytometry in vaginal lavages

from women with vulvovaginitis and normal microflora. *Am J Reprod Immunol.* 2012;67(3):198-205.

40. Kyongo JK, Jespers V, Goovaerts O, Michiels J, Menten J, Fichorova RN, et al. Searching for lower female genital tract soluble and cellular biomarkers: defining levels and predictors in a cohort of healthy Caucasian women. *PLoS One.* 2012;7(8):e43951.

41. Anahtar MN, Byrne EH, Doherty KE, Bowman BA, Yamamoto HS, Soumillon M, et al. Cervicovaginal bacteria are a major modulator of host inflammatory responses in the female genital tract. *Immunity.* 2015;42(5):965-76.

42. Hedges SR, Barrientes F, Desmond RA, and Schwebke JR. Local and systemic cytokine levels in relation to changes in vaginal flora. *J Infect Dis.* 2006;193(4):556-62.

43. Byrne EH, Farcasanu M, Bloom SM, Xulu N, Xu J, Hykes BL, Jr., et al. Antigen Presenting Cells Link the Female Genital Tract Microbiome to Mucosal Inflammation, With Hormonal Contraception as an Additional Modulator of Inflammatory Signatures. *Front Cell Infect Microbiol.* 2021;11:733619.

44. Qulu WP, Mzobe G, Mtshali A, Letsoalo MP, Osman F, San JE, et al. Metronidazole Treatment Failure and Persistent BV Lead to Increased Frequencies of Activated T- and Dendritic-Cell Subsets. *Microorganisms.* 2023;11(11).

45. Hughes SM, Ferre AL, Yandura SE, Shetler C, Baker CAR, Calienes F, et al. Cryopreservation of human mucosal tissues. *PLoS One.* 2018;13(7):e0200653.

46. Lund JM, Hladik F, and Prlic M. Advances and challenges in studying the tissue-resident T cell compartment in the human female reproductive tract. *Immunol Rev.* 2023;316(1):52-62.

47. Nguyen TH, Kumar D, Prince C, Martini D, Grunwell JR, Lawrence T, et al. Frequency of HLA-DR(+)CD38(hi) T cells identifies and quantifies T-cell activation in hemophagocytic lymphohistiocytosis, hyperinflammation, and immune regulatory disorders. *J Allergy Clin Immunol.* 2024;153(1):309-19.

48. Hay ZLZ, and Slansky JE. Granzymes: The Molecular Executors of Immune-Mediated Cytotoxicity. *Int J Mol Sci.* 2022;23(3).

49. Fang F, Yu M, Cavanagh MM, Hutter Saunders J, Qi Q, Ye Z, et al. Expression of CD39 on Activated T Cells Impairs their Survival in Older Individuals. *Cell Rep.* 2016;14(5):1218-31.

50. Xu L, Cao Y, Xie Z, Huang Q, Bai Q, Yang X, et al. The transcription factor TCF-1 initiates the differentiation of T(FH) cells during acute viral infection. *Nat Immunol.* 2015;16(9):991-9.

51. Choi YS, Gullicksrud JA, Xing S, Zeng Z, Shan Q, Li F, et al. LEF-1 and TCF-1 orchestrate T(FH) differentiation by regulating differentiation circuits upstream of the transcriptional repressor Bcl6. *Nat Immunol.* 2015;16(9):980-90.

52. Wu T, Shin HM, Moseman EA, Ji Y, Huang B, Harly C, et al. TCF1 Is Required for the T Follicular Helper Cell Response to Viral Infection. *Cell Rep.* 2015;12(12):2099-110.

53. Yang BH, Wang K, Wan S, Liang Y, Yuan X, Dong Y, et al. TCF1 and LEF1 Control Treg Competitive Survival and Tfr Development to Prevent Autoimmune Diseases. *Cell Rep.* 2019;27(12):3629-45 e6.

54. Yu Q, Sharma A, Oh SY, Moon HG, Hossain MZ, Salay TM, et al. T cell factor 1 initiates the T helper type 2 fate by inducing the transcription factor GATA-3 and repressing interferon-gamma. *Nat Immunol.* 2009;10(9):992-9.

55. Zhang J, He Z, Sen S, Wang F, Zhang Q, and Sun Z. TCF-1 Inhibits IL-17 Gene Expression To Restrain Th17 Immunity in a Stage-Specific Manner. *J Immunol.* 2018;200(10):3397-406.

56. Zhang J, Lyu T, Cao Y, and Feng H. Role of TCF-1 in differentiation, exhaustion, and memory of CD8(+) T cells: A review. *FASEB J.* 2021;35(5):e21549.

57. Feinen B, Jerse AE, Gaffen SL, and Russell MW. Critical role of Th17 responses in a murine model of Neisseria gonorrhoeae genital infection. *Mucosal Immunol.* 2010;3(3):312-21.

58. Masson L, Salkinder AL, Olivier AJ, McKinnon LR, Gamieldien H, Mlisana K, et al. Relationship between female genital tract infections, mucosal interleukin-17 production and local T helper type 17 cells. *Immunology.* 2015;146(4):557-67.

59. Acosta-Rodriguez EV, Rivino L, Geginat J, Jarrossay D, Gattorno M, Lanzavecchia A, et al. Surface phenotype and antigenic specificity of human interleukin 17-producing T helper memory cells. *Nat Immunol.* 2007;8(6):639-46.

60. Annunziato F, Cosmi L, Liotta F, Maggi E, and Romagnani S. The phenotype of human Th17 cells and their precursors, the cytokines that mediate their differentiation and the role of Th17 cells in inflammation. *Int Immunol.* 2008;20(11):1361-8.

61. McKinnon LR, and Kaul R. Quality and quantity: mucosal CD4+ T cells and HIV susceptibility. *Curr Opin HIV AIDS.* 2012;7(2):195-202.

62. Josefowicz SZ, Lu LF, and Rudensky AY. Regulatory T cells: mechanisms of differentiation and function. *Annu Rev Immunol.* 2012;30:531-64.

63. Groom JR, and Luster AD. CXCR3 in T cell function. *Exp Cell Res.* 2011;317(5):620-31.

64. McMichael AJ, and Rowland-Jones SL. Cellular immune responses to HIV. *Nature.* 2001;410(6831):980-7.

65. Brenna E, and McMichael AJ. The Importance of Cellular Immune Response to HIV: Implications for Antibody Production and Vaccine Design. *DNA Cell Biol.* 2022;41(1):38-42.

66. Schey R, Dornhoff H, Baier JL, Purtak M, Opoka R, Koller AK, et al. CD101 inhibits the expansion of colitogenic T cells. *Mucosal Immunol.* 2016;9(5):1205-17.

67. Hudson WH, Gensheimer J, Hashimoto M, Wieland A, Valanparambil RM, Li P, et al. Proliferating Transitory T Cells with an Effector-like Transcriptional Signature Emerge from PD-1(+) Stem-like CD8(+) T Cells during Chronic Infection. *Immunity.* 2019;51(6):1043-58 e4.

68. Minnie SA, Waltner OG, Zhang P, Takahashi S, Nemychenkov NS, Ensbey KS, et al. TIM-3(+) CD8 T cells with a terminally exhausted phenotype retain functional capacity in hematological malignancies. *Sci Immunol.* 2024;9(94):eadg1094.

69. Philip M, Fairchild L, Sun L, Horste EL, Camara S, Shakiba M, et al. Chromatin states define tumour-specific T cell dysfunction and reprogramming. *Nature.* 2017;545(7655):452-6.

70. Joag VR, McKinnon LR, Liu J, Kidane ST, Yudin MH, Nyanga B, et al. Identification of preferential CD4+ T-cell targets for HIV infection in the cervix. *Mucosal Immunol.* 2016;9(1):1-12.

71. Stieh DJ, Matias E, Xu H, Fought AJ, Blanchard JL, Marx PA, et al. Th17 Cells Are Preferentially Infected Very Early after Vaginal Transmission of SIV in Macaques. *Cell Host Microbe.* 2016;19(4):529-40.

72. Cantero-Perez J, Grau-Exposito J, Serra-Peinado C, Rosero DA, Luque-Ballesteros L, Astorga-Gamaza A, et al. Resident memory T cells are a cellular reservoir for HIV in the cervical mucosa. *Nat Commun.* 2019;10(1):4739.

73. Khader SA, Pearl JE, Sakamoto K, Gilmartin L, Bell GK, Jelley-Gibbs DM, et al. IL-23 compensates for the absence of IL-12p70 and is essential for the IL-17 response during tuberculosis but is dispensable for protection and antigen-specific IFN-gamma responses if IL-12p70 is available. *J Immunol.* 2005;175(2):788-95.

74. Tang C, Chen S, Qian H, and Huang W. Interleukin-23: as a drug target for autoimmune inflammatory diseases. *Immunology.* 2012;135(2):112-24.

75. Foucher ED, Blanchard S, Preisser L, Descamps P, Ifrah N, Delneste Y, et al. IL-34- and M-CSF-induced macrophages switch memory T cells into Th17 cells via membrane IL-1alpha. *Eur J Immunol.* 2015;45(4):1092-102.

76. Cao W, Yang Y, Wang Z, Liu A, Fang L, Wu F, et al. Leukemia inhibitory factor inhibits T helper 17 cell differentiation and confers treatment effects of neural progenitor cell therapy in autoimmune disease. *Immunity.* 2011;35(2):273-84.

77. Gulzar N, and Copeland KF. CD8+ T-cells: function and response to HIV infection. *Curr HIV Res.* 2004;2(1):23-37.

78. Collins DR, Gaiha GD, and Walker BD. CD8(+) T cells in HIV control, cure and prevention. *Nat Rev Immunol.* 2020;20(8):471-82.

79. Phares TW, Stohlman SA, Hwang M, Min B, Hinton DR, and Bergmann CC. CD4 T cells promote CD8 T cell immunity at the priming and effector site during viral encephalitis. *J Virol.* 2012;86(5):2416-27.

80. Joag V, Obila O, Gajer P, Scott MC, Dizzell S, Humphrys M, et al. Impact of Standard Bacterial Vaginosis Treatment on the Genital Microbiota, Immune Milieu, and Ex Vivo Human Immunodeficiency Virus Susceptibility. *Clin Infect Dis.* 2019;68(10):1675-83.

81. Serebrenik J, Wang T, Hunte R, Srinivasan S, McWalters J, Tharp GK, et al. Differences in Vaginal Microbiota, Host Transcriptome, and Proteins in Women With Bacterial Vaginosis Are Associated With Metronidazole Treatment Response. *J Infect Dis.* 2021;224(12):2094-104.

82. Shannon B, Gajer P, Yi TJ, Ma B, Humphrys MS, Thomas-Pavanel J, et al. Distinct Effects of the Cervicovaginal Microbiota and Herpes Simplex Type 2 Infection on Female Genital Tract Immunology. *J Infect Dis.* 2017;215(9):1366-75.

83. Vestergaard C, Deleuran M, Gesser B, and Larsen CG. Thymus- and activation-regulated chemokine (TARC/CCL17) induces a Th2-dominated inflammatory reaction on intradermal injection in mice. *Exp Dermatol.* 2004;13(4):265-71.

84. Imai T, Nagira M, Takagi S, Kakizaki M, Nishimura M, Wang J, et al. Selective recruitment of CCR4-bearing Th2 cells toward antigen-presenting cells by the CC chemokines thymus and activation-regulated chemokine and macrophage-derived chemokine. *Int Immunol.* 1999;11(1):81-8.

85. Walker JA, and McKenzie ANJ. T(H)2 cell development and function. *Nat Rev Immunol.* 2018;18(2):121-33.

86. Kokubo K, Onodera A, Kiuchi M, Tsuji K, Hirahara K, and Nakayama T. Conventional and pathogenic Th2 cells in inflammation, tissue repair, and fibrosis. *Front Immunol.* 2022;13:945063.

87. Conroy DM, and Williams TJ. Eotaxin and the attraction of eosinophils to the asthmatic lung. *Respir Res.* 2001;2(3):150-6.

88. Crump MP, Gong JH, Loetscher P, Rajarathnam K, Amara A, Arenzana-Seisdedos F, et al. Solution structure and basis for functional activity of stromal cell-derived factor-1; dissociation of CXCR4 activation from binding and inhibition of HIV-1. *EMBO J.* 1997;16(23):6996-7007.

89. Amara A, Gall SL, Schwartz O, Salamero J, Montes M, Loetscher P, et al. HIV coreceptor downregulation as antiviral principle: SDF-1alpha-dependent internalization of the chemokine receptor CXCR4 contributes to inhibition of HIV replication. *J Exp Med.* 1997;186(1):139-46.

90. Signoret N, Oldridge J, Pelchen-Matthews A, Klasse PJ, Tran T, Brass LF, et al. Phorbol esters and SDF-1 induce rapid endocytosis and down modulation of the chemokine receptor CXCR4. *J Cell Biol.* 1997;139(3):651-64.

91. Losikoff P, Fichorova R, Snyder B, Rodriguez I, Cu-Uvin S, Harwell J, et al. Genital tract interleukin-8 but not interleukin-1beta or interleukin-6 concentration is associated with bacterial vaginosis and its clearance in HIV-infected and HIV-uninfected women. *Infect Dis Obstet Gynecol.* 2007;2007:92307.

92. Mtshali A, San JE, Osman F, Garrett N, Balle C, Giandhari J, et al. Temporal Changes in Vaginal Microbiota and Genital Tract Cytokines Among South African Women Treated for Bacterial Vaginosis. *Front Immunol.* 2021;12:730986.

93. Nugent RP, Krohn MA, and Hillier SL. Reliability of diagnosing bacterial vaginosis is improved by a standardized method of gram stain interpretation. *J Clin Microbiol.* 1991;29(2):297-301.

94. Golden MR, Ashley-Morrow R, Swenson P, Hogrefe WR, Handsfield HH, and Wald A. Herpes simplex virus type 2 (HSV-2) Western blot confirmatory testing among men testing positive for HSV-2 using the focus enzyme-linked immunosorbent assay in a sexually transmitted disease clinic. *Sex Transm Dis.* 2005;32(12):771-7.

95. Laeyendecker O, Henson C, Gray RH, Nguyen RH, Horne BJ, Wawer MJ, et al. Performance of a commercial, type-specific enzyme-linked immunosorbent assay for detection of herpes simplex virus type 2-specific antibodies in Ugandans. *J Clin Microbiol.* 2004;42(4):1794-6.

96. Gamiel JL, Tobian AA, Laeyendecker OB, Reynolds SJ, Morrow RA, Serwadda D, et al. Improved performance of enzyme-linked immunosorbent assays and the effect of human immunodeficiency virus coinfection on the serologic detection of herpes simplex virus type 2 in Rakai, Uganda. *Clin Vaccine Immunol.* 2008;15(5):888-90.

97. Lingappa J, Nakku-Joloba E, Magaret A, Friedrich D, Dragavon J, Kambugu F, et al. Sensitivity and specificity of herpes simplex virus-2 serological assays among HIV-infected and uninfected urban Ugandans. *Int J STD AIDS.* 2010;21(9):611-6.

98. Mujugira A, Morrow RA, Celum C, Lingappa J, Delany-Moretlwe S, Fife KH, et al. Performance of the Focus HerpeSelect-2 enzyme immunoassay for the detection of herpes simplex virus type 2 antibodies in seven African countries. *Sex Transm Infect.* 2011;87(3):238-41.

99. Amsel R, Totten PA, Spiegel CA, Chen KC, Eschenbach D, and Holmes KK. Nonspecific vaginitis. Diagnostic criteria and microbial and epidemiologic associations. *Am J Med.* 1983;74(1):14-22.

100. Segerer S, Mac KM, Regele H, Kerjaschki D, and Schlondorff D. Expression of the C-C chemokine receptor 5 in human kidney diseases. *Kidney Int.* 1999;56(1):52-64.

101. McKean JW, and Hettmansperger TP. A Robust Analysis of the General Linear Model Based on One Step R- Estimates. *Biometrika.* 1978;65(3):571-9.

Figure 1

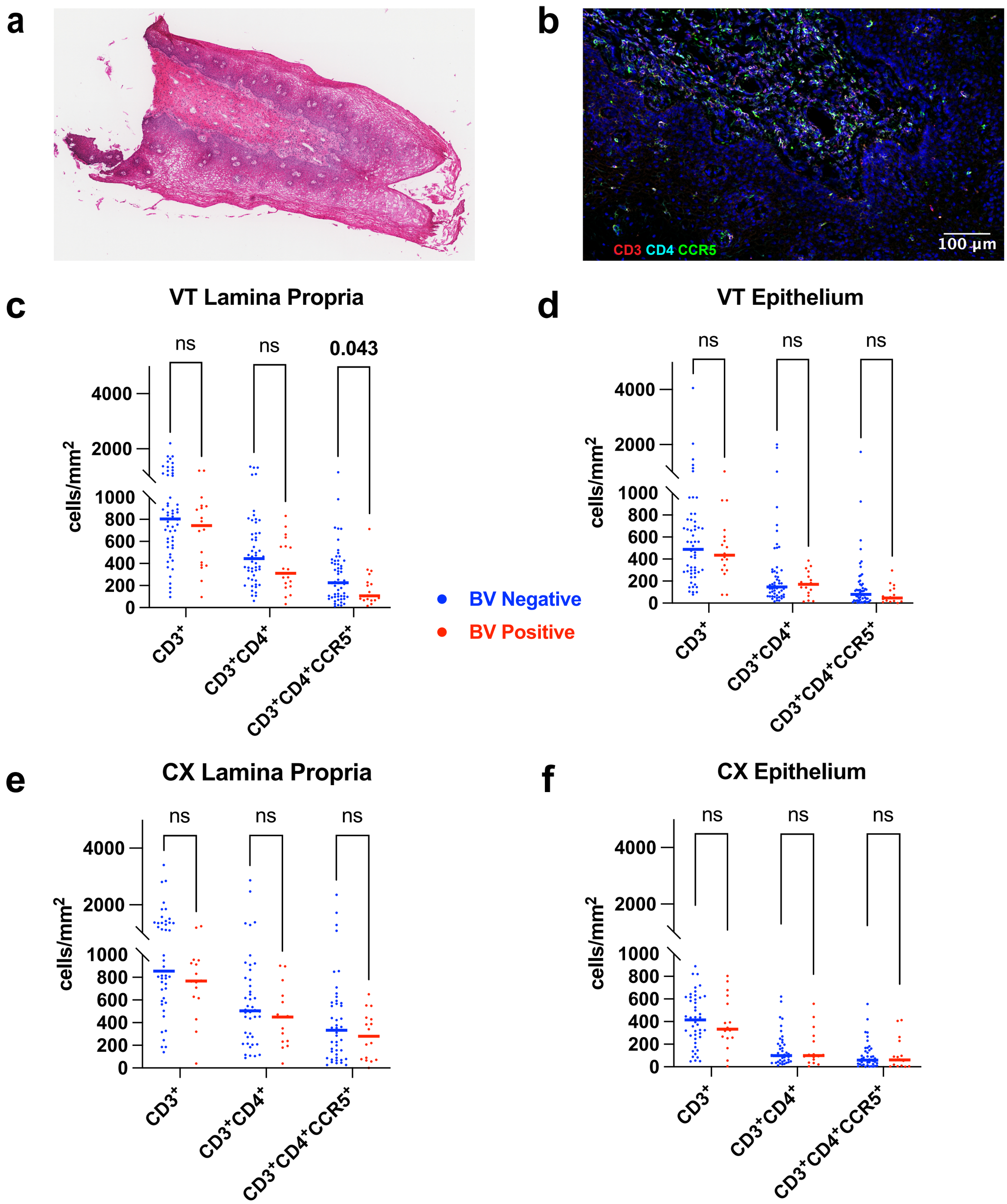
a
b
CD3 CD4 CCR5
100 µm
c
VT Lamina Propria
ns
ns
0.043
cells/mm2
4000
2000
1000
800
600
400
200
0
CD3+
CD3+CD4+
CD3+CD4+CCR5+
BV Negative
BV Positive
d
VT Epithelium
ns
ns
ns
e
CX Lamina Propria
f
CX Epithelium

Figure 2

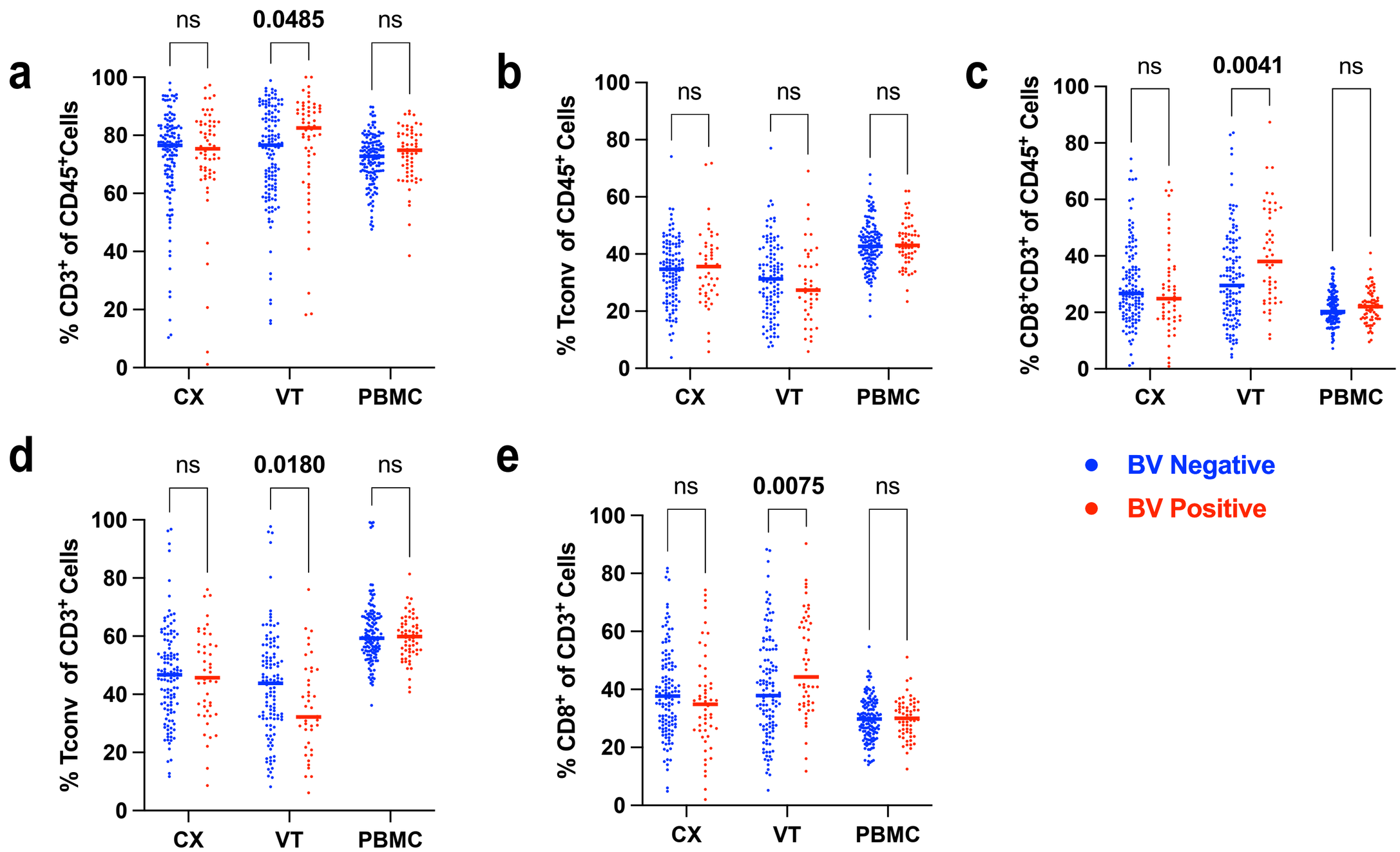
a
b
c
d
e
ns
0.0485
0.0041
0.0180
0.0075
% CD3+ of CD45+Cells
% Tconv of CD45+ Cells
% CD8+CD3+ of CD45+ Cells
% Tconv of CD3+ Cells
% CD8+ of CD3+ Cells
0
20
40
60
80
100
CX
VT
PBMC
BV Negative
BV Positive

Figure 3

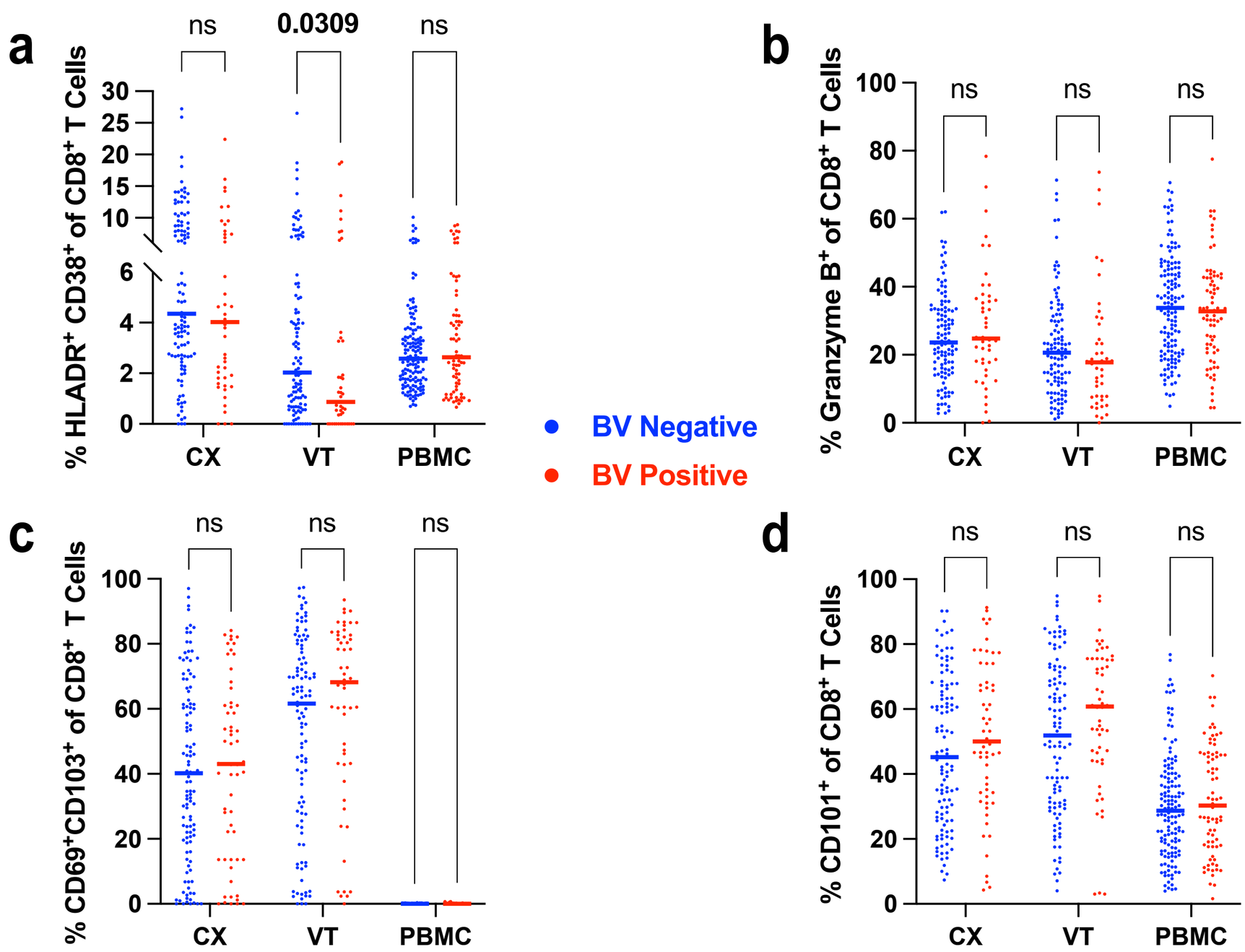
a
ns
0.0309
ns
% HLADR+ CD38+ of CD8+ T Cells
30
25
20
15
10
6
4
2
0
CX
VT
PBMC
BV Negative
BV Positive
b
% Granzyme B+ of CD8+ T Cells
100
80
60
40
20
0
ns
ns
ns
CX
VT
PBMC
c
% CD69+CD103+ of CD8+ T Cells
100
80
60
40
20
0
ns
ns
ns
CX
VT
PBMC
d
% CD101+ of CD8+ T Cells
100
80
60
40
20
0
ns
ns
ns
CX
VT
PBMC

Figure 4

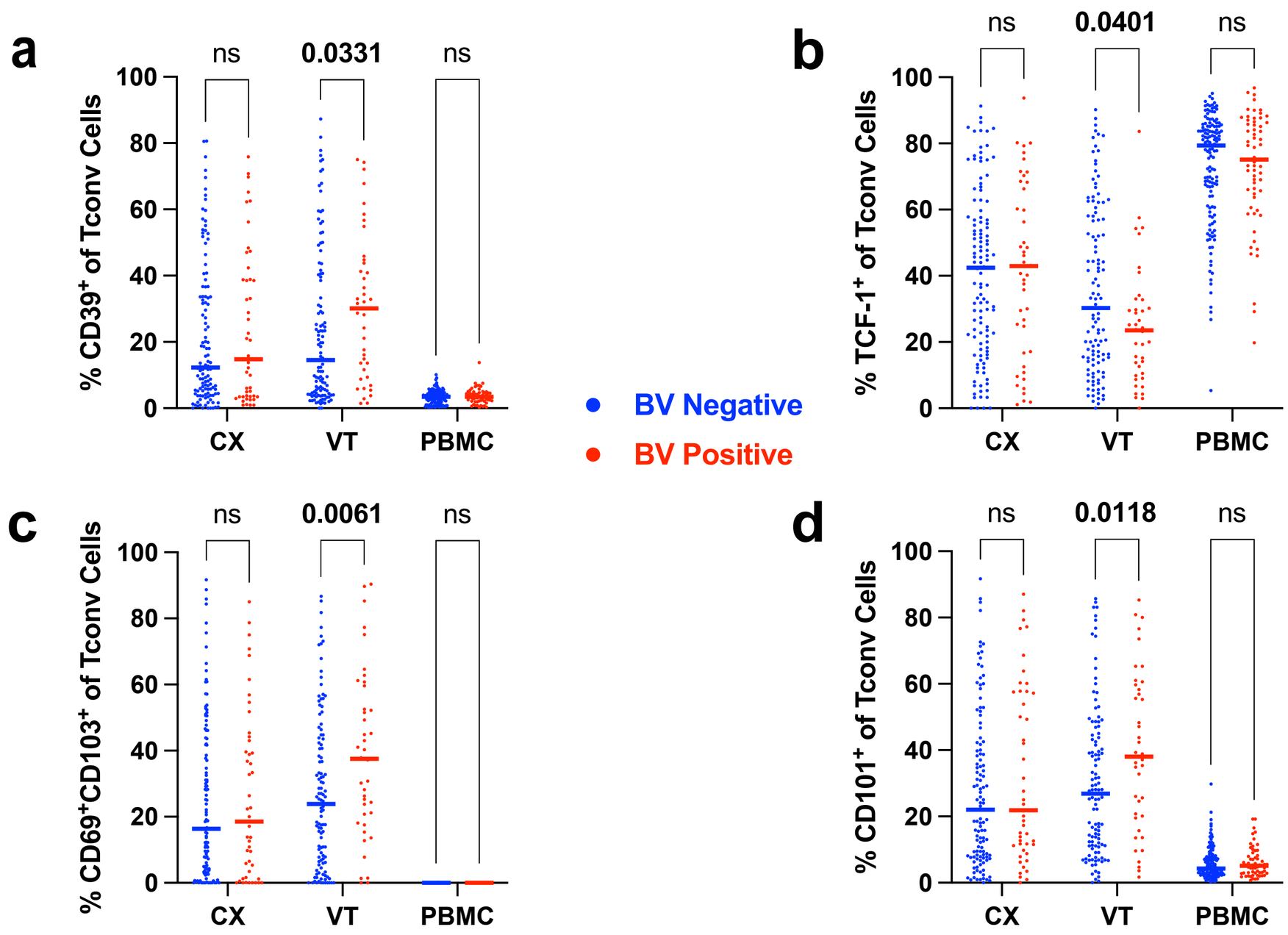
a
% CD39+ of Tconv Cells
ns
0.0331
ns
CX
VT
PBMC
b
% TCF-1+ of Tconv Cells
ns
0.0401
ns
CX
VT
PBMC
BV Negative
BV Positive
c
% CD69+CD103+ of Tconv Cells
ns
0.0061
ns
CX
VT
PBMC
d
% CD101+ of Tconv Cells
ns
0.0118
ns
CX
VT
PBMC

Figure 5

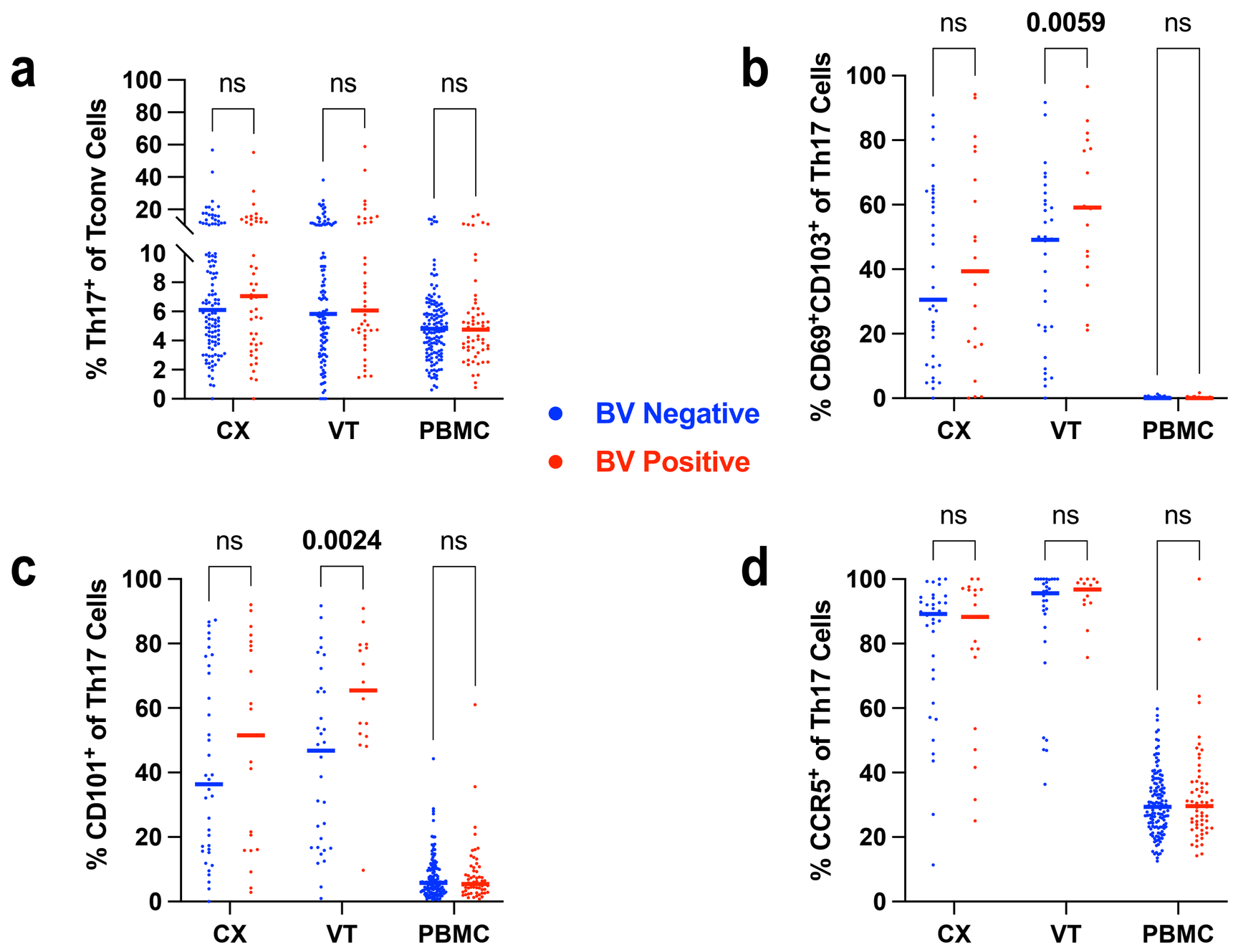
a
% Th17+ of Tconv Cells
100
80
60
40
20
10
8
6
4
2
0
ns
ns
ns
CX
VT
PBMC
b
% CD69+CD103+ of Th17 Cells
ns
0.0059
ns
c
% CD101+ of Th17 Cells
ns
0.0024
ns
d
% CCR5+ of Th17 Cells
ns
ns
ns
BV Negative
BV Positive

Figure 6

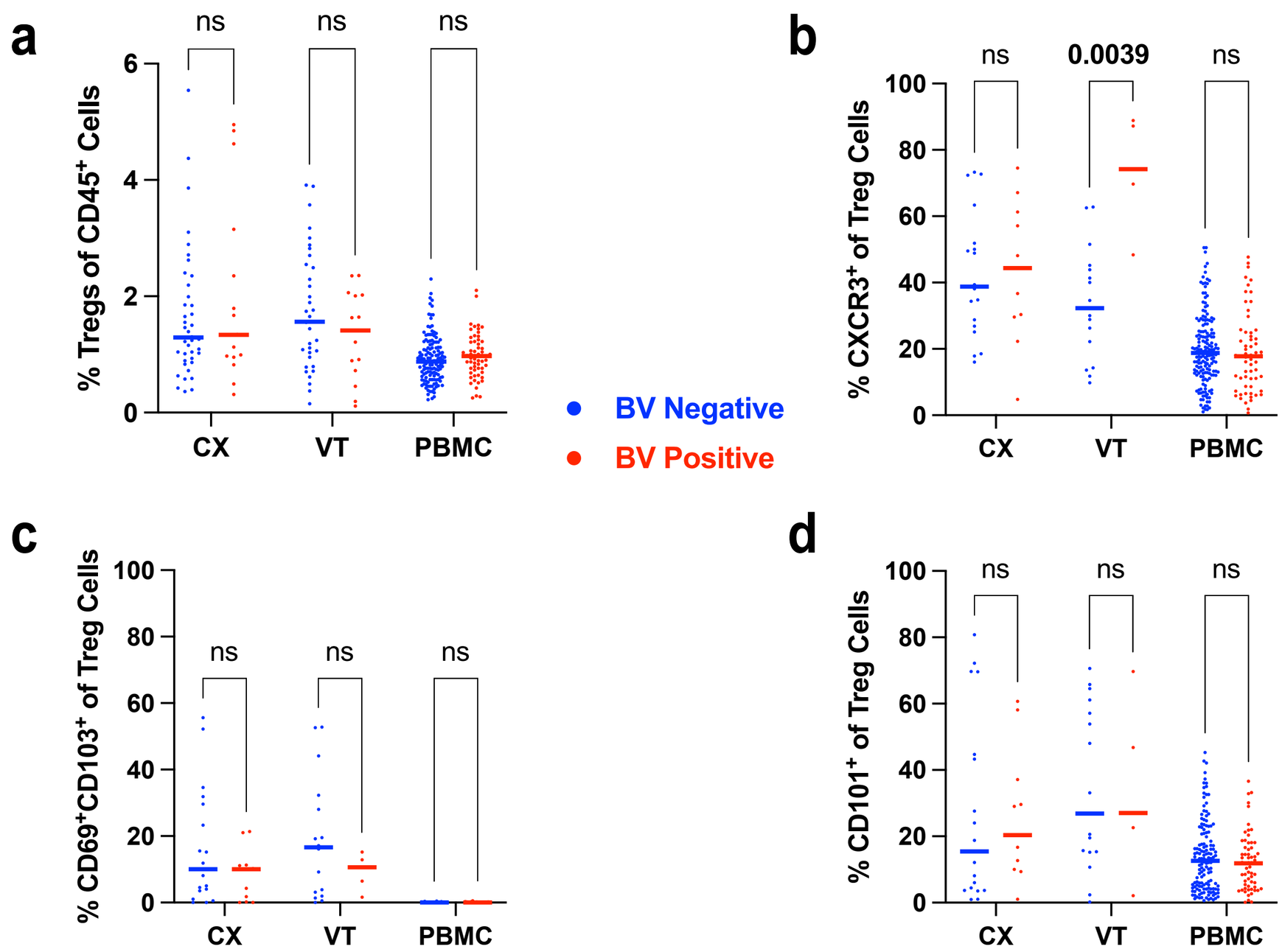
a
% Tregs of CD45+ Cells
ns
ns
ns
CX
VT
PBMC
b
% CXCR3+ of Treg Cells
ns
0.0039
ns
CX
VT
PBMC
BV Negative
BV Positive
c
% CD69+CD103+ of Treg Cells
ns
ns
ns
CX
VT
PBMC
d
% CD101+ of Treg Cells
ns
ns
ns
CX
VT
PBMC

Figure 7

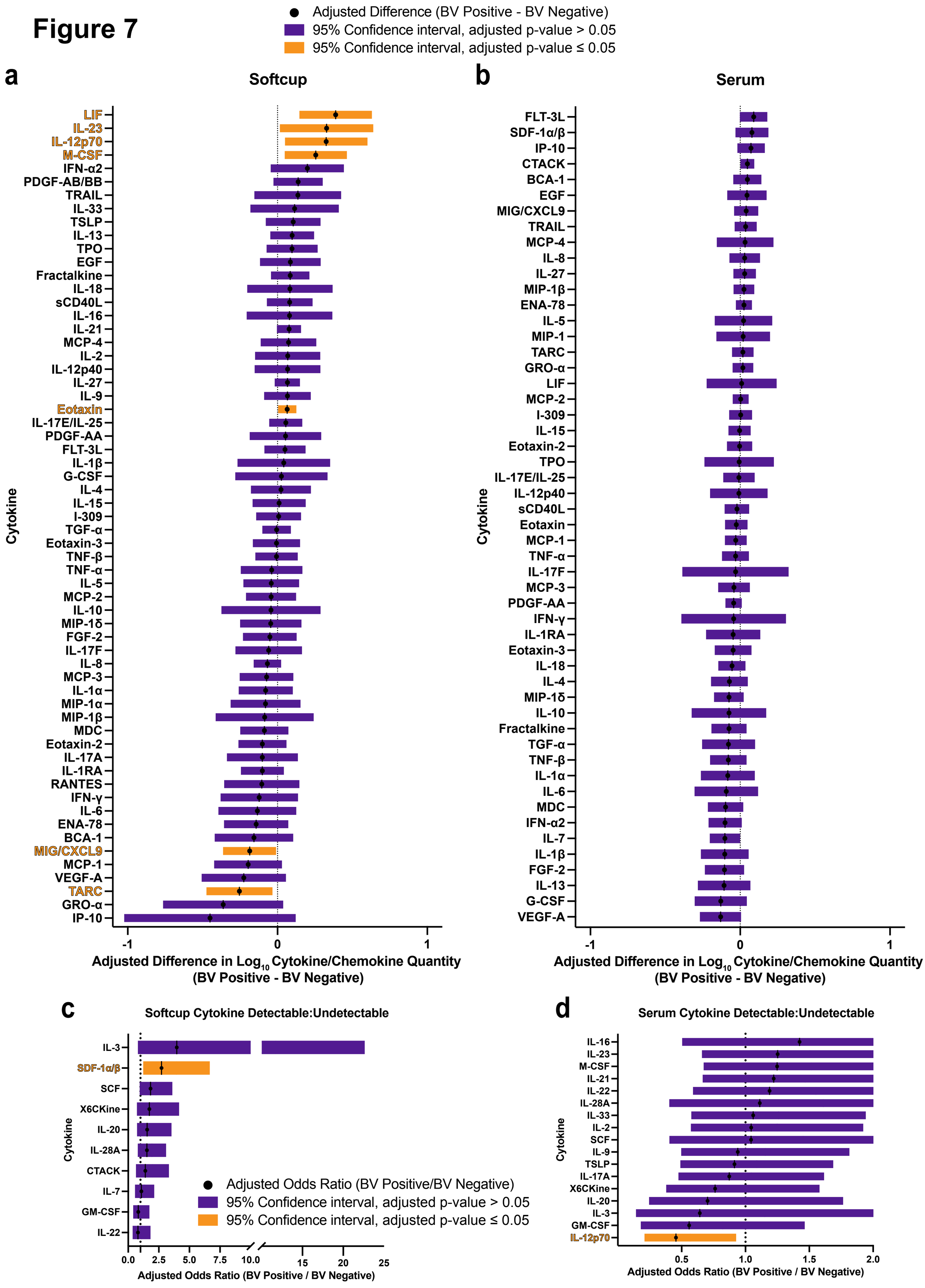
Adjusted Difference (BV Positive - BV Negative)
95% Confidence interval, adjusted p-value > 0.05
95% Confidence interval, adjusted p-value ≤ 0.05
a
Softcup
LIF
IL-23
IL-12p70
M-CSF
IFN-α2
PDGF-AB/BB
TRAIL
IL-33
TSLP
IL-13
TPO
EGF
Fractalkine
IL-18
sCD40L
IL-16
IL-21
MCP-4
IL-2
IL-12p40
IL-27
IL-9
Eotaxin
IL-17E/IL-25
PDGF-AA
FLT-3L
IL-1β
G-CSF
IL-4
IL-15
I-309
TGF-α
Eotaxin-3
TNF-β
TNF-α
IL-5
MCP-2
IL-10
MIP-1δ
FGF-2
IL-17F
IL-8
MCP-3
IL-1α
MIP-1α
MIP-1β
MDC
Eotaxin-2
IL-17A
IL-1RA
RANTES
IFN-γ
IL-6
ENA-78
BCA-1
MIG/CXCL9
MCP-1
VEGF-A
TARC
GRO-α
IP-10
Cytokine
-1
0
1
Adjusted Difference in Log10 Cytokine/Chemokine Quantity
(BV Positive - BV Negative)
b
Serum
FLT-3L
SDF-1α/β
IP-10
CTACK
BCA-1
EGF
MIG/CXCL9
TRAIL
MCP-4
IL-8
IL-27
MIP-1β
ENA-78
IL-5
MIP-1
TARC
GRO-α
LIF
MCP-2
I-309
IL-15
Eotaxin-2
TPO
IL-17E/IL-25
IL-12p40
sCD40L
Eotaxin
MCP-1
TNF-α
IL-17F
MCP-3
PDGF-AA
IFN-γ
IL-1RA
Eotaxin-3
IL-18
IL-4
MIP-1δ
IL-10
Fractalkine
TGF-α
TNF-β
IL-1α
IL-6
MDC
IFN-α2
IL-7
IL-1β
FGF-2
IL-13
G-CSF
VEGF-A
Cytokine
-1
0
1
Adjusted Difference in Log10 Cytokine/Chemokine Quantity
(BV Positive - BV Negative)
c
Softcup Cytokine Detectable:Undetectable
IL-3
SDF-1α/β
SCF
X6CKine
IL-20
IL-28A
CTACK
IL-7
GM-CSF
IL-22
Cytokine
Adjusted Odds Ratio (BV Positive/BV Negative)
95% Confidence interval, adjusted p-value > 0.05
95% Confidence interval, adjusted p-value ≤ 0.05
0.0
2.5
5.0
7.5
10.0
15
20
25
Adjusted Odds Ratio (BV Positive / BV Negative)
d
Serum Cytokine Detectable:Undetectable
IL-16
IL-23
M-CSF
IL-21
IL-22
IL-28A
IL-33
IL-2
SCF
IL-9
TSLP
IL-17A
X6CKine
IL-20
IL-3
GM-CSF
IL-12p70
Cytokine
0.5
1.0
1.5
2.0
Adjusted Odds Ratio (BV Positive / BV Negative)

Table 1 – Demographic and Clinical Characteristics

BV Status	Overall N = 212[1]	Negative N = 148[1]	Positive N = 64[1]
Age			
<=24	69 (33%)	51 (34%)	18 (28%)
25-29	50 (24%)	31 (21%)	19 (30%)
30-34	35 (17%)	27 (18%)	8 (13%)
35-39	29 (14%)	18 (12%)	11 (17%)
40-49	26 (12%)	20 (14%)	6 (9.4%)
>=50	3 (1.4%)	1 (0.7%)	2 (3.1%)
HIV Exposure			
HIV exposed (HIV serodifferent couple)	37 (17%)	25 (17%)	12 (19%)
HIV unexposed (HIV negative, concordant couple)	175 (83%)	123 (83%)	52 (81%)
HSV-2 Status			
Indeterminate	9 (4.2%)	8 (5.4%)	1 (1.6%)
Seronegative	118 (56%)	91 (61%)	27 (42%)
Not done	2 (0.9%)	1 (0.7%)	1 (1.%)
Seropositive	83 (39%)	48 (32%)	35 (55%)
Hormonal Contraceptive Use			
Had menses in last 35 days	93 (45%)	64 (44%)	29 (48%)
Secondary amenorrhea	32 (15%)	21 (14%)	11 (18%)
Uses hormonal contraceptives	82 (40%)	62 (42%)	20 (33%)
Missing	5	1	4
Number of unprotected vaginal intercourse in last 30 days	8 (3,12)	8 (4,12)	8 (1,12)

[1]n (%); Median (IQR)